Regulation by cyclic-di-GMP attenuates dynamics and enhances robustness of bimodal curli gene activation in *Escherichia coli*

Olga Lamprecht[1#†], Maryia Ratnikava[1#], Paulina Jacek[1], Eugen Kaganovitch[1], Nina Buettner[1], Kirstin Fritz[1], Ina Biazruchka[1], Robin Köhler[1], Julian Pietsch[1], and Victor Sourjik[1*]

[1]Max Planck Institute for Terrestrial Microbiology and Center for Synthetic Microbiology (SYNMIKRO), Karl-von-Frisch Strasse 14, 35043 Marburg, Germany

[#]These authors contributed equally to this work

[†]Present address: Eawag: Swiss Federal Institute of Aquatic Science and Technology, Dübendorf, Switzerland

*Corresponding author: Victor Sourjik, victor.sourjik@synmikro.mpi-marburg.mpg.de

Abstract

Curli amyloid fibers are a major constituent of the extracellular biofilm matrix formed by bacteria of the Enterobacteriaceae family. Within *Escherichia coli* biofilms, curli gene expression is limited to a subpopulation of bacteria, leading to heterogeneity of extracellular matrix synthesis. Here we show that bimodal activation of curli expression occurs not only in submerged and macrocolony biofilms, but also in well-mixed planktonic cultures of *E. coli*, resulting in all-or-none stochastic differentiation into distinct subpopulations of curli-positive and curli-negative cells at the entry into the stationary phase of growth. Stochastic curli activation in individual *E. coli* cells could further be observed during continuous growth in a conditioned medium in a microfluidic device, which further revealed that the curli-positive state is only metastable. In agreement with previous reports, regulation of curli gene expression by c-di-GMP via two pairs of diguanylate cyclase and phosphodiesterase enzymes, DgcE/PdeH and DgcM/PdeR, modulates the fraction of curli-positive cells under all tested growth conditions. Unexpectedly, removal of this regulatory network does not abolish the bimodality of curli gene expression, although it affects dynamics of activation and increases heterogeneity of expression levels among individual cells. Moreover, the fraction of curli-positive cells within an *E. coli* population shows stronger dependence on growth conditions in the absence of c-di-GMP regulation. We thus conclude that, while not required for the emergence of bimodal curli gene expression in *E. coli*, this c-di-GMP regulatory network attenuates the frequency and dynamics of gene activation and increases its robustness to cellular heterogeneity and environmental variation.

Keywords: Gene expression, bacteria, biofilm, bistability, differentiation, amyloid fibers

Introduction

Curli amyloid fibers are the key component of the extracellular matrix produced during biofilm formation by *Escherichia coli*, *Salmonella enterica*, and other Enterobacteriaceae [1-9]. In *E. coli* and *S. enterica* serovar Typhimurium, curli genes are organized in two divergently transcribed *csgBAC* and *csgDEFG* operons that share a common intergenic regulatory region [10]. Expression of these operons is under regulation of the stationary phase sigma factor σ^S (RpoS) and thus becomes activated during the entry into the stationary phase of growth [4, 11-14]. This activation is achieved by the σ^S-dependent induction of the transcriptional regulator CsgD, which then controls the expression of the *csgBAC* operon that encodes the major curli subunit CsgA along with the curli nucleator CsgB and the chaperone CsgC [7, 8, 15]. In turn, *csgD* expression in *E. coli* and *S.* Typhimurium is either directly or indirectly regulated by multiple cellular factors that mediate responses to diverse environmental changes, including both global and specific transcriptional regulators, small regulatory RNAs and second messengers (reviewed in [16-19]).

One of the key regulators of *csgD* is the transcription factor MlrA [13, 14, 20, 21]. The activity of MlrA depends on cellular levels of bacterial second messenger bis-(3'-5')-cyclic dimeric guanosine monophosphate (c-di-GMP), and in *E. coli* this control is known to be mediated by a pair of the interacting diguanylate cyclase (DGC) and phosphodiesterase (PDE) enzymes, DgcM and PdeR, that form a ternary complex with MlrA [12, 14, 22]. MlrA is kept inactive by binding PdeR, and this interaction is relieved when the latter becomes active as a PDE thus acting as the trigger enzyme [22, 23]. This inhibition is counteracted both by DgcM, which locally produces c-di-GMP to engage PdeR, as well as by the global pool of c-di-GMP. Besides its enzymatic activity, DgcM might also activate MlrA through direct protein interaction. Another DGC-PDH pair, DgcE and PdeH, provides global regulatory input into the local DgcM-PdeR-MlrA regulation [12, 24]. At least under typical conditions used to study *E. coli* biofilms, this regulatory network appears to be the only c-di-GMP-dependent input that controls *csgD* expression [24].

Previous studies of *E. coli* macrocolony biofilms formed on agar plates showed that curli expression occurs in the upper layer of the colony, but even in this layer its expression remained heterogeneous [25-27], indicating an interplay between global regulation of curli gene expression by microenvironmental gradients within biofilms and its inherent stochasticity. Differentiation of *E. coli* into distinct subpopulations of cells either expressing or not expressing curli was also observed in submerged biofilms formed in liquid cultures, whereby curli expression was associated with cellular aggregation [28]. Furthermore, bi- or multimodality of *csgD* reporter activity was also observed in the early stationary phase among planktonic cells in *S.* Typhimurium [29, 30] and *E. coli* [27]. Given established c-di-GMP-dependent regulation of CsgD activity, it was proposed that bistable curli expression originates from a toggle switch

created by mutual inhibition between DgcM and PdeR, which could act as a bistable switch on *csgD* gene expression [27, 31].

In this study we demonstrate that differentiation of *E. coli csgBAC* operon expression, leading to formation of distinct subpopulations of curli-positive and -negative cells, occurs not only in submerged and macrocolony biofilms but also stochastically in a well-stirred planktonic culture and thus in the absence of any environmental gradients. Similar stochastic and reversible differentiation could be further observed among cells growing in conditioned medium in the microfluidic device. Although the c-di-GMP regulatory network consisting of the DgcE/PdeH and DgcM/PdeR pairs modulates the fraction of curli-positive cells in the population and the dynamics and uniformity of curli gene activation, it is not required to establish the bimodality of their expression.

Materials and methods

Bacterial strains and plasmids

All strains and plasmids used in this study are listed in Table S1. A derivative of *E. coli* W3110 [26] that was engineered to encode a chromosomal transcriptional sfGFP reporter downstream of the *csgA* gene [28] (VS1146) was used here as the wild-type strain. Gene deletions were obtained with the help of P1 phage transduction using strains of the Keio collection [32] as donors, and the kanamycin resistance cassette was removed using FLP recombinase [33]. For expression, *dgcE* and *pdeH* genes were cloned into the pTrc99A vector [34].

Growth conditions for planktonic cultures

Planktonic *E. coli* cultures were grown in tryptone broth (TB) medium (10 g tryptone, 5 g NaCl per liter, pH 7.0) or lysogeny broth (LB) medium without salt (10 g tryptone, 5 g yeast extract, per liter, pH 7.0), supplemented with antibiotics where necessary. Overnight cultures were inoculated from LB agar plates, grown at 30°C and diluted 1:100, unless indicated otherwise, in 5-10 ml of fresh TB and grown at 30°C at 200 rpm in 100 ml flasks in a rotary shaker until the indicated OD_{600} or overnight (18-25 h; OD_{600} ~ 1.3-1.8). Alternatively, cultures were grown in TB in 96-well plates with orbital shaking in a plate reader, with 200 µl culture per well. Where indicated, bacterial cultures were supplemented with either 1 mM L-serine (after 6 h of growth) or 0.1–10 mg/l DL-serine hydroxamate at inoculation.

Growth and quantification of submerged biofilms

Submerged biofilms were grown and quantified as described previously [28], with minor modifications. Overnight bacterial cultures grown in TB were diluted 1:100 in fresh TB medium and grown at 200 rpm and 30°C in a rotary shaker to OD_{600} of 0.5. The cultures were then diluted in fresh TB medium to a final OD_{600} of 0.05, and 300 µl was loaded into a 96-well plate

111 (Corning Costar, flat bottom; Sigma-Aldrich, Germany) and incubated without shaking at 30°C
112 for 46 h.
113 For quantification of biofilm formation, the non-attached cells were removed and the wells were
114 washed once with phosphate-buffered saline (PBS; 8 g NaCl, 0.2 g KCl, 1.44 g Na_2HPO_4, 0.24
115 g KH_2PO_4). Attached cells were fixed for 20 min with 300 µl of 96% ethanol, allowed to dry for
116 40 min, and stained with 300 µl of 0.1% crystal violet (CV) solution for 15 min at room
117 temperature. The wells were subsequently washed twice with 1x PBS, incubated with 300 µl
118 of 96% ethanol for 35 min and the CV absorption was measured at OD_{595} using INFINITE M
119 $NANO^+$ plate reader (Tecan Group Ltd., Switzerland). Obtained CV values were normalized to
120 the OD_{600} values of the respective biofilm cultures.
121
122 **Macrocolony biofilm assay**
123 Macrocolony biofilms were grown as described previously [26]. Briefly, 5 µl of the overnight
124 liquid culture grown at 37°C in LB medium (10 g tryptone, 5 g NaCl, and 5 g yeast extract per
125 liter) was spotted on salt-free LB agar plates supplemented with Congo red (40 µg/ml). Plates
126 were incubated for 8 days at 28°C.
127
128 **Fluorescence measurements**
129 Measurements of GFP expression in an INFINITE M1000 PRO plate reader (Tecan Group
130 Ltd., Switzerland) were done using fluorescence excitation at 483 nm and emission at 535 nm.
131 Relative fluorescence was calculated by normalizing to corresponding OD_{600} values of the
132 culture.
133 For fluorescence measurements using flow cytometry, aliquots of 40-300 µl of liquid bacterial
134 cultures were mixed with 2 ml of tethering buffer (10 mM KH_2PO_4, 10 mM K_2HPO_4, 0.1 mM
135 EDTA, 1 µM L-methionine, 10 mM lactic acid, pH 7.0). Macrocolonies were collected from the
136 plate, resuspended in 10 ml of tethering buffer and then aliquots of 40 µl were mixed with 2 ml
137 of fresh tethering buffer. Samples were vigorously vortexed and then immediately subjected to
138 flow cytometric analysis using BD LSRFortessa Sorp cell analyzer (BD Biosciences, Germany)
139 using 488-nm laser. In each experimental run, 50,000 individual cells were analyzed. Absence
140 of cell aggregation was confirmed by using forward scatter (FSC) and side scatter (SSC)
141 parameters. Data were analyzed using FlowJo software version v10.7.1 (FlowJo LLC,
142 Ashland, OR, US).
143
144 **Microfluidics**
145 Conditioned medium was prepared by cultivating wild-type *E. coli* in TB in a rotary shaker at
146 30°C for 20 h, after which the cell suspension was centrifuged at 4000 rpm for 10 min, medium
147 was filter-sterilized and stored at 4°C. Mother machine [35] microfluidics devices were

148 designed, fabricated and operated as described in Supporting protocols. *E. coli* cells from the
149 overnight culture in TB were loaded into the mother machine by manual infusion of the cell
150 suspension through one of the two inlets using a 1-ml syringe. Cells were first allowed to grow
151 at 30 °C for 4 h in fresh TB, then switched to the conditioned TB and cultivated for up to 26 h.
152 Phase contrast and GFP fluorescence images were acquired using a Nikon Eclipse Ti-E
153 inverted microscope with a time interval of 10 min. Details of image analysis are described in
154 Supporting protocols.
155

156 ## Results

157 **Bimodal curli gene expression is induced in planktonic culture**

158 In order to characterize curli expression in planktonic culture of *E. coli*, we followed the
159 induction of a chromosomal transcriptional reporter for the *csgBAC* operon, where the gene
160 encoding for stable green fluorescent protein (GFP) was cloned downstream of *csgA* with a
161 strong ribosome binding site as part of the same polycistronic RNA [28]. In our previous study
162 of submerged *E. coli* biofilms, this reporter showed bimodal expression both in the surface-
163 attached biofilm and in the pellicle at the liquid-air interface, and its activity correlated with the
164 recruitment of individual cells into multicellular aggregates [28]. When *E. coli* culture was grown
165 at 30°C in tryptone broth (TB) liquid medium, this reporter became induced during the transition
166 to stationary phase (Figure 1A), which is consistent with previous reports [12, 14, 27]. The GFP
167 reporter level remains high in the stationary phase, which also explains its initially high
168 fluorescence in our plate reader experiments, where the culture is inoculated using stationary-
169 phase cells. The observed induction of curli expression occurred at similar densities in the
170 cultures with different initial inoculum size. In both cases the onset of induction apparently
171 coincided with the reduction of the growth rate, which might occur due to depletion of amino
172 acids in the medium and induction of the stringent response [36, 37], consistent with the
173 proposed role of the stringent response in the regulatory cascade leading to curli gene
174 expression [18, 23]. In agreement with that, curli expression was strongly reduced when *E. coli*
175 cultures were grown in a concentrated TB medium (Figure S1A) or when TB medium was
176 supplemented with serine (Figure S2A). Moreover, curli reporter induction was enhanced by
177 the addition of serine hydroxamate (SHX), which is known to mimic amino acid starvation and
178 induce the stringent response [38] (Figure S2A).
179 In order to investigate whether curli expression was uniform or heterogeneous within
180 planktonic *E. coli* populations, we next measured curli reporter activity in individual cells using
181 flow cytometry. The reporter was induced only in a fraction of cells, and this bimodality of curli
182 expression became increasingly more pronounced at later stages of culture growth, reaching
183 its maximum in the overnight culture (Figure 1B). Thus, the bimodal induction of curli gene
184 expression is observed not only in biofilms but also in well-mixed planktonic cultures. Upon

185 inspection of the flask culture by microscopy, no cell aggregation could be observed,
186 suggesting that curli gene induction in a subpopulation of bacteria is not due to the formation
187 of suspended biofilm-like aggregates [39]. While curli activation was more pronounced in a cell
188 culture growing in an orbital shaker in a flask (Figure 1B), bimodality was also observed for
189 cultures grown in a plate reader (Figure S1B and Figure S2B). Notably, stimulation of curli
190 expression by SHX, or its suppression by additional nutrients, affected the fraction of positive
191 cells rather than their expression levels (Figure S1B and Figure S2B).
192
193 **Bimodality of curli gene expression does not require the known c-di-GMP regulatory**
194 **network**
195 Subsequently, we investigated dependence of bimodal activation of curli gene expression in
196 planktonic culture on the known regulation of curli expression in *E. coli* by the global (DgcE
197 and PdeH) and local (DgcM and PdeR) pairs of DGC/PDE enzymes [12, 14, 22] (Figure 2A).
198 In agreement with this model of c-di-GMP-dependent regulation, activation of curli reporter
199 was completely abolished in the absence of MlrA (Figure 2B), and it was strongly reduced by
200 deletions of *dgcE* and *dgcM* and enhanced by deletions of *pdeH* and *pdeR* genes (Figure 2C).
201 Notably, under these conditions a small fraction of curli-positive cells could still be detected in
202 cultures of both DGC gene deletion strains, and a small fraction of curli-negative cells was
203 observed for both PDE gene deletion strains, indicating that deletions of these genes do not
204 eliminate the bimodality of curli gene expression or its levels in curli-positive cells but rather
205 change the probability of curli genes to become activated in individual cells.
206 Consistently, bimodality was also retained upon combined deletions of pairs of DGC/PDE
207 genes. Removal of the entire global level of c-di-GMP regulation led to a bimodal pattern of
208 curli reporter activation within the population of Δ*pdeH* Δ*dgcE* cells (Figure 2D) that was similar
209 to that observed in the wild-type culture, despite a smaller fraction of curli-positive cells in the
210 deletion strain. Even more surprisingly, the distribution of curli reporter expression remained
211 bimodal upon removal of the local level of c-di-GMP regulation in Δ*pdeR* Δ*dgcM* strain,
212 although the fraction of curli-positive cells was reduced in this background, too.
213 We observed that level of curli gene expression in Δ*pdeR* Δ*dgcM* strain was lower than in
214 Δ*pdeR* strain, which confirms that DgcM can promote curli expression independently of PdeR
215 [12, 14, 22] (Figure 2A). This conclusion is further supported by the comparison between the
216 triple deletion strain Δ*pdeH* Δ*dgcE* Δ*pdeR* that expresses only DgcM (Figure 2E) and the
217 quadruple deletion strain Δ*pdeH* Δ*dgcE* Δ*pdeR* Δ*dgcM* that lacks the entire regulatory network
218 (Figure 2F), with much higher fraction of culri-positive cells observed in the former background.
219 Most importantly, the bimodality of curli expression was still observed in the quadruple deletion
220 strain (Figure 2F).

221 We thus conclude that, whereas the known c-di-GMP-dependent regulation of MlrA activity
222 does clearly affect the fraction of curli-positive cells, it is not required to establish bimodality of
223 curli gene expression in the planktonic cell population. The network has further only little impact
224 of the level of curli reporter activity in individual positive cells (i.e., on position of the positive
225 peak in the flow cytometry data), although reporter intensity in positive cells appeared to be
226 slightly reduced in the strains lacking DgcM.
227 *Vibrio cholerae* transcriptional regulator VpsT, a close homologue of CsgD, has been shown
228 to be directly regulated by binding to c-di-GMP [40]. Furthermore, in both *S.* Typhimurium and
229 *E. coli*, curli gene expression might also be regulated by c-di-GMP independently of *csgD*
230 transcription [41-43]. We thus aimed to examine whether *E. coli* curli gene expression was no
231 longer sensitive to the global cellular level of c-di-GMP in the absence of the local PdeR/DgcM
232 regulatory module. Indeed, whereas the overexpression of DgcE or of PdeH, which both affect
233 the global pool of c-di-GMP in *E. coli*, had strong impacts on the fraction of curli-positive cells
234 in the wild type, the quadruple mutant was insensitive to such overexpression (Figure 3). This
235 result suggests that in this background, the expression of the *csgBAC* reporter is indeed no
236 longer affected by global c-di-GMP levels. This further excludes regulation by other DGCs that
237 contribute to the common c-di-GMP pool, although it does not rule out hypothetical regulation
238 by a local DGC/PDE pair that is insensitive to global c-di-GMP levels.
239
240 **Curli gene activation shows higher growth-condition dependent variability in the**
241 **absence of the c-di-GMP regulatory network**
242 We next explored how the fraction of curli-positive cells in the population depends on the
243 conditions of culture growth, with or without regulation by c-di-GMP. As noted above, when
244 the wild-type *E. coli* culture was grown in multi-well plates, both the fraction of curli-positive
245 cells and the level of reporter activity in positive cells were moderately reduced compared to
246 incubation in a flask in an orbital shaker (Figure 2B, Figure 4A and Figure S1B). The reduction
247 in the number of curli-positive cells under these growth conditions was even more pronounced
248 for Δ*pdeR* Δ*dgcM* or Δ*pdeH* Δ*dgcE* Δ*pdeR* Δ*dgcM* strains (Figure 4A and Figure S3), where
249 only a small fraction of cells (12%) became positive, compared to 40-50% in the flask culture
250 (Figure 2D,F). Interestingly, this difference was less for the Δ*pdeH* Δ*dgcE* strain (24% vs 30%).
251 Deletions of individual DGC or PDE genes generally showed expected phenotypes, but
252 fractions of curli-positive cells in Δ*pdeH* and Δ*pdeR* strains were again reduced compared with
253 flask cultures (Figure 2C). Another notable difference between flask and multi-well plate
254 cultures was that the low-fluorescence peak of the wild-type culture was not fully negative but
255 apparently contained a large fraction of cells with incompletely activated curli reporter, which
256 could also be seen in the Δ*pdeH* or Δ*pdeR* strains but not in the Δ*pdeH* Δ*dgcE* Δ*pdeR* Δ*dgcM,*
257 Δ*pdeR* Δ*dgcM* or Δ*pdeH* Δ*dgcE* strains. Similar results were obtained even upon prolonged

258 incubation in the plate reader (Figure S4), confirming that the observed difference with the
259 overnight flask culture was not because of the different growth stage but rather due to
260 differences in growth conditions.
261 We further tested reporter activation under growth conditions that favor biofilm formation.
262 During formation of static submerged biofilms in multi-well plates, where cultures are grown
263 without shaking, the overall curli activation pattern in cell populations of individual or double
264 and quadruple deletion strains (Figure 4B) was comparable to that in the flask culture grown
265 in the orbital shaker (Figure 2B-D, F), although effects of DGC and PDE gene deletions on the
266 fraction of curli-positive cells were apparently reduced. Curli gene activation in individual
267 mutant strains correlated well with the levels of submerged biofilm formation (Figure S5), but
268 the lack of regulation by c-di-GMP resulted in stronger reduction of the biofilm biomass than
269 simply expected from its effect on curli gene expression, consistent with additional roles of c-
270 di-GMP in biofilm formation.
271 All strains were also grown in the form of macrocolony biofilms on agar plates containing the
272 salt-free LB medium, as done previously [26] (Figure 4C), as well as in the liquid salt-free LB
273 medium as a control (Figure 4D). Expression of curli reporter in individual cells within the
274 macrocolony was analyzed by flow cytometry immediately after colony resuspension (see
275 Materials and Methods), so that the level of stable GFP reporter should reflect cell-specific
276 curli expression within the macrocolony. The overall dependency of reporter activation on the
277 deletions of individual DGC and PDE genes was again qualitatively similar to other growth
278 conditions (Figure 4C). However, the fraction of curli-positive cells in the macrocolony biofilms
279 was less sensitive to deletions of individual *dgc* or *pdh* genes than in planktonic cultures,
280 regardless whether the latter were grown in TB (Figure 2C) or in the salt-free LB (Figure 4D).
281 This agrees with stronger Congo red staining of macrocolonies of Δ*dgcE* and Δ*dgcM* strains
282 compared to the Δ*mlrA* negative control (Figure S6). Thus, during macrocolony biofilm
283 formation, regulation by c-di-GMP appears to be less important for the activation of curli gene
284 expression, possibly because other regulators contribute to this activation in a highly structured
285 environment. Importantly, the curli-positive cell fraction in both macrocolony and planktonic
286 cultures of Δ*pdeR* Δ*dgcM* and Δ*pdeH* Δ*dgcE* Δ*pdeR* Δ*dgcM* strains growing on the salt-free LB
287 was much higher than under other growth conditions.
288 To summarize, under all of the tested growth conditions, regulation by the known c-di-GMP
289 regulatory network was not required for bimodal curli activation, although it indeed affected the
290 fraction of curli-positive cells. Nevertheless, the absence of this c-di-GMP control apparently
291 makes the fraction of curli-positive cells in the population more sensitive to environmental
292 conditions, since this fraction exhibited much larger variation in the quadruple deletion
293 compared to the wild-type strain among different growth conditions tested here.
294

295 **Dynamics and variability of stochastic curli gene activation in individual cells is**
296 **controlled by the c-di-GMP regulatory network**
297 In order to investigate the dynamics of curli gene activation, and the impact of c-di-GMP
298 regulation, at the single-cell level, we utilized a “mother machine” device — a microfluidic chip
299 where growth of individual bacterial cell lineages could be followed in a highly parallelized
300 manner over multiple generations [35] (Figure 5 and Supporting protocols). Since our design
301 of the mother machine allows rapid switching of the medium supplied to the cells (Figure 5D),
302 we could mimic nutrient depletion in order to activate curli expression in continuously growing
303 single cells. For that, wild-type, individual DGC or PDE, or quadruple deletion strains were first
304 loaded into the mother machine from overnight cultures, allowed to grow in fresh TB medium
305 for several generations, and then shifted to the TB medium that was pre-conditioned by
306 growing a batch culture (see Materials and Methods and Supporting protocols). A fraction of
307 curli-positive cells was observed at the beginning of these experiments, which was strain-
308 specific and consistent with the expected fraction of positive cells in the overnight cultures of
309 each respective strain. After resuming exponential growth in the fresh medium all cells turned
310 off curli expression (Figure 6A,C, Figure S7 and Movie S1, Movie S2 and Movie S3). Following
311 the shift to conditioned medium, cell growth rate was strongly reduced (Figure 6E and Figure
312 S8), and after several generations of slow growth, individual cells of all strains activated curli
313 expression, while other cells remained in the curli-off state (Figure 6A,C,F, Figure S7 and
314 Movie S1, Movie S2 and Movie S3). Importantly, the frequencies of curli-positive cells in
315 individual mutants were consistent with those of the planktonic cultures, confirming that the
316 overall control of curli gene expression by the c-di-GMP regulatory network is similar for growth
317 in conditioned medium in the mother machine.
318 Although the overall frequency of curli reporter activation was comparable for the wild-type and
319 Δ*pdeH* Δ*dgcE* Δ*pdeR* Δ*dgcM* cells lacking c-di-GMP regulatory network, we further compared
320 the dynamics of single-cell curli activation in both backgrounds. First, we observed that, in both
321 strains, curli reporter activation was transient — and after several generations in the curli-on
322 state individual cells turned curli expression off again during continuous growth in the
323 conditioned medium (Figure 6B,D, Figure S8 and Figure S9). In some cases, the initial
324 transient pulse of activation was even followed by a second activation event. Although such
325 transient curli reporter activation was observed in both backgrounds, with a similar delay after
326 exposure to conditioned medium (Figure 6H), its dynamics showed several important
327 differences between strains. Most clearly, the rate of curli activation in individual cells was
328 higher in the absence of the c-di-GMP-regulatory network (Figure 6G,I and Figure S10A,B),
329 which led to stronger but more transient increase in their fluorescence (Figure 6J,K and Figure
330 S10B). Additionally, the level of reporter induction showed greater intercellular heterogeneity
331 in the Δ*pdeH* Δ*dgcE* Δ*pdeR* Δ*dgcM* strain (Figure 6,D,J, Figure S9). Thus, the control of curli

332 expression by c-di-GMP reduces the rate but also the cell-to-cell variability of curli induction
333 within population.
334

335 **Discussion**

336 Expression of the curli biofilm matrix genes is known to be heterogeneous or even bistable in
337 communities of *E. coli* [25-28] and *S.* Typhimurium [29, 30], which might have important
338 functional consequences for the biomechanics of bacterial biofilms [27] and for stress
339 resistance and virulence of bacterial populations [29, 30]. In the well-structured macrocolony
340 biofilms, differentiation into subpopulations with different levels of curli matrix production is
341 largely deterministic and driven by gradients of nutrients and oxygen [18], but bimodality of
342 curli expression might also emerge stochastically, in a well-mixed population or between cells
343 within the same layer of a macrocolony [27, 29, 30]. How this bimodality originates within the
344 extremely complex regulatory network of curli genes [17, 19, 23, 27] remains a matter of
345 debate. Although earlier work proposed that bistable expression of curli might be a
346 consequence of positive transcriptional feedback in *csgD* regulation [30, 44], the most recently
347 suggested model attributed bistability to the properties of the c-di-GMP regulatory switch
348 formed by DgcM, PdeR and MlrA [27, 31]. Furthermore, although this bimodal pattern of curli
349 gene expression has typically been referred to as bistable, temporal dynamics and stability of
350 its induction in individual cells has not been directly investigated.
351 Here, we studied the expression of the major curli *csgBAC* operon in well-stirred planktonic *E.*
352 *coli* cultures as well as in submerged and macrocolony biofilms and during growth in a
353 microfluidics device. Consistent with previous studies [12, 14, 27], the induction of curli gene
354 expression in growing *E. coli* cell populations was observed during entry into the stationary
355 phase of growth. Curli activation was apparently dependent on depletion of nutrients, most
356 likely amino acids, since it could be suppressed by increasing the levels of nutrients or, more
357 specifically, by addition of serine, and conversely, it could be enhanced by the SHX-mediated
358 stimulation of the stringent response. We further observed that activation of the *csgBAC*
359 operon exhibited strongly pronounced bimodality under all tested conditions, resulting in two
360 distinct, curli-positive and -negative, subpopulations of cells even in a well-stirred planktonic
361 culture. Stochastic bimodality of curli reporter activation was confirmed in a microfluidic device,
362 where, following shift to conditioned medium, only a fraction of the cell population turned on
363 curli gene expression.
364 Such differentiation is apparently consistent with previous reports of bimodal *csgD* expression
365 in the stationary phase of *S.* Typhimurium [29, 30] and *E. coli* [27] culture growth. However, in
366 contrast with the previous interpretation of such a *csgD* expression pattern as bistability, we
367 observed that activation of curli gene expression during continuous cell growth in the
368 microfluidic device was only transient and unstable. Moreover, our data indicate that the

369 bimodality of the *csgBAC* expression is unlikely to be (fully) explained by the bimodal
370 expression of *csgD*. Firstly, compared to the bimodality of the *csgBAC* reporter, the previously
371 reported bimodality of *csgD* expression in *E. coli* [27] was much less pronounced and became
372 apparent only in later stages of planktonic culture growth. Moreover, in that study, all wild-type
373 cells showed activation of the *csgD* reporter, differing only in the level of this activation, which
374 itself cannot explain the on/off bimodality of the *csgBAC* reporter activation.
375 Secondly, and most importantly, whereas the bimodality of *csgD* expression was observed to
376 be dependent on regulation by the DgcE/PdeH/DgcM/PdeR network [27], this was clearly not
377 the case for *csgBAC* reporter expression. Under all tested conditions, including planktonic
378 cultures, submerged and macrocolony biofilms, and growth in the microfluidic device, the
379 differentiation into distinct subpopulations of positive and negative cells in our experiments
380 occurred in the absence of this entire c-di-GMP regulatory network. Since removal of the
381 DgcM/PdeR module further made curli gene expression insensitive to global levels of c-di-
382 GMP, contributions of other *E. coli* DGCs and PDEs to curli regulation in this deletion
383 background are unlikely, even if these enzymes might in principle affect curli gene expression
384 in wild-type *E. coli* cells via the common c-di-GMP pool. We therefore conclude that c-di-GMP
385 regulation might be dispensable for activation or bimodality of curli gene expression in *E. coli*,
386 although we could not rule out regulation of curli gene expression by a hypothetical local
387 DGC/PDE module that is insensitive to global c-di-GMP levels.
388 Nevertheless, c-di-GMP control clearly plays an important role during the establishment of
389 bimodality. Consistent with previous studies, we observed that the DGC and PDE proteins
390 determine the fraction of curli-positive cells [22, 23, 27], although they have no or only little
391 effect on the average level of *csgBAC* expression in individual cells. Our results further suggest
392 that the DgcE/PdeH/DgcM/PdeR regulatory network might make curli expression in *E. coli*
393 populations more robust, helping to ensure that the fraction of curli-positive cells is less
394 variable under different culture growth conditions. This might be related to the observed effect
395 of this network on the temporal expression dynamics in a continuously growing culture, with
396 faster but more heterogeneous activation of curli expression in the absence of the c-di-GMP
397 control, although whether and how there two different kinds of variability and their suppression
398 by are connected remains to be investigated. It is further possible that the increased
399 robustness provided by c-di-GMP regulation is due to the network-induced bimodality of *csgD*
400 expression discussed above [27], which might provide an additional stabilizing feedback.
401 How might the observed pulsatile activation of the curli-positive state originate at the single-
402 cell level and lead to the differentiation into distinct subpopulations in *E. coli* culture? Pulsing
403 in expression was proposed to be common to many gene regulatory circuits [45, 46, 47]. It was
404 recently described in *E. coli* for the upstream regulator of curli, σ^S [48], as well as for the
405 flagellar regulon [49, 50] that is anti-regulated with curli [28]. However, in neither of these cases

did pulsing lead to bimodality of expression, and their relation to the observed pulses in curli expression thus remains to be seen.

Regardless of the origin of pulsatile expression, the timing and duration of curli activation pulses can explain how such transient activation leads to differentiation into two distinct subpopulations in the planktonic culture. Since the curli expression is only turned on during transition to the stationary phase, individual cells stochastically activate curli genes just before the culture growth ceases, thus making subsequent reversion to the curli-negative state impossible. Although curli gene regulation in biofilms might be more complex, spatial stratification of gene expression in the macrocolony biofilms was proposed to resemble the temporal regulation of expression in planktonic cultures [18, 26]. Thus, also in this case, curli activation would happen in a cell layer just before it ceases to grow, fixing the differentiation between curli-positive and curli-negative cells within this colony layer.

Acknowledgements

We thank Sarah Hoch, Silvia González Sierra and Gabriele Malengo for technical help and advice.

References

1. Arnqvist A, Olsen A, Pfeifer J, Russell DG, Normark S. The Crl protein activates cryptic genes for curli formation and fibronectin binding in *Escherichia coli* HB101. Mol Microbiol. 1992;6(17):2443-52. Epub 1992/09/01. doi: 10.1111/j.1365-2958.1992.tb01420.x. PubMed PMID: 1357528.
2. Hufnagel DA, Depas WH, Chapman MR. The Biology of the *Escherichia coli* Extracellular Matrix. Microbiol Spectr. 2015;3(3). Epub 2015/07/18. doi: 10.1128/microbiolspec.MB-0014-2014. PubMed PMID: 26185090; PubMed Central PMCID: PMCPMC4507285.
3. Larsen P, Nielsen JL, Dueholm MS, Wetzel R, Otzen D, Nielsen PH. Amyloid adhesins are abundant in natural biofilms. Environmental Microbiology. 2007. doi: 10.1111/j.1462-2920.2007.01418.x.
4. Romling U, Bian Z, Hammar M, Sierralta WD, Normark S. Curli fibers are highly conserved between *Salmonella typhimurium* and *Escherichia coli* with respect to operon structure and regulation. J Bacteriol. 1998;180(3):722-31. Epub 1998/02/11. doi: 10.1128/JB.180.3.722-731.1998. PubMed PMID: 9457880; PubMed Central PMCID: PMCPMC106944.
5. Vidal O, Longin R, Prigent-Combaret C, Dorel C, Hooreman M, Lejeune P. Isolation of an *Escherichia coli* K-12 mutant strain able to form biofilms on inert surfaces: involvement of a new ompR allele that increases curli expression. J Bacteriol. 1998;180(9):2442-9. Epub 1998/05/09. doi: 10.1128/JB.180.9.2442-2449.1998. PubMed PMID: 9573197; PubMed Central PMCID: PMCPMC107187.
6. Zogaj X, Bokranz W, Nimtz M, Romling U. Production of cellulose and curli fimbriae by members of the family Enterobacteriaceae isolated from the human gastrointestinal tract.

447 Infect Immun. 2003;71(7):4151-8. Epub 2003/06/24. doi: 10.1128/IAI.71.7.4151-4158.2003.
448 PubMed PMID: 12819107; PubMed Central PMCID: PMCPMC162016.
449 7. Tursi SA, Tukel C. Curli-Containing Enteric Biofilms Inside and Out: Matrix Composition,
450 Immune Recognition, and Disease Implications. Microbiol Mol Biol Rev. 2018;82(4). Epub
451 2018/10/12. doi: 10.1128/MMBR.00028-18. PubMed PMID: 30305312; PubMed Central
452 PMCID: PMCPMC6298610.
453 8. Chapman MR, Robinson LS, Pinkner JS, Roth R, Heuser J, Hammar M, et al. Role of
454 *Escherichia coli* curli operons in directing amyloid fiber formation. Science.
455 2002;295(5556):851-5. Epub 2002/02/02. doi: 10.1126/science.1067484. PubMed PMID:
456 11823641; PubMed Central PMCID: PMCPMC2838482.
457 9. Dueholm MS, Albertsen M, Otzen D, Nielsen PH. Curli Functional Amyloid Systems Are
458 Phylogenetically Widespread and Display Large Diversity in Operon and Protein Structure.
459 PLoS ONE. 2012. doi: 10.1371/journal.pone.0051274.
460 10. Gerstel U, Römling U. The csgD promoter, a control unit for biofilm formation in
461 *Salmonella typhimurium*. Research in Microbiology2003.
462 11. Brombacher E, Baratto A, Dorel C, Landini P. Gene expression regulation by the Curli
463 activator CsgD protein: modulation of cellulose biosynthesis and control of negative
464 determinants for microbial adhesion. J Bacteriol. 2006;188(6):2027-37. Epub 2006/03/04. doi:
465 10.1128/JB.188.6.2027-2037.2006. PubMed PMID: 16513732; PubMed Central PMCID:
466 PMCPMC1428138.
467 12. Pesavento C, Becker G, Sommerfeldt N, Possling A, Tschowri N, Mehlis A, et al. Inverse
468 regulatory coordination of motility and curli-mediated adhesion in *Escherichia coli*. Genes Dev.
469 2008;22(17):2434-46. Epub 2008/09/04. doi: 10.1101/gad.475808. PubMed PMID: 18765794;
470 PubMed Central PMCID: PMCPMC2532929.
471 13. Romling U, Rohde M, Olsen A, Normark S, Reinkoster J. AgfD, the checkpoint of
472 multicellular and aggregative behaviour in *Salmonella typhimurium* regulates at least two
473 independent pathways. Mol Microbiol. 2000;36(1):10-23. Epub 2000/04/12. doi:
474 10.1046/j.1365-2958.2000.01822.x. PubMed PMID: 10760159.
475 14. Weber H, Pesavento C, Possling A, Tischendorf G, Hengge R. Cyclic-di-GMP-mediated
476 signalling within the sigma network of *Escherichia coli*. Mol Microbiol. 2006;62(4):1014-34.
477 Epub 2006/10/03. doi: 10.1111/j.1365-2958.2006.05440.x. PubMed PMID: 17010156.
478 15. Barnhart MM, Chapman MR. Curli biogenesis and function. Annu Rev Microbiol.
479 2006;60:131-47. Epub 2006/05/18. doi: 10.1146/annurev.micro.60.080805.142106. PubMed
480 PMID: 16704339; PubMed Central PMCID: PMCPMC2838481.
481 16. Ishihama A. Prokaryotic genome regulation: Multifactor promoters, multitarget
482 regulators and hierarchic networks. FEMS Microbiology Reviews2010.
483 17. Rossi E, Cimdins A, Luthje P, Brauner A, Sjoling A, Landini P, et al. "It's a gut feeling" -
484 *Escherichia coli* biofilm formation in the gastrointestinal tract environment. Crit Rev Microbiol.
485 2018;44(1):1-30. Epub 2017/05/10. doi: 10.1080/1040841X.2017.1303660. PubMed PMID:
486 28485690.
487 18. Serra DO, Hengge R. Bacterial Multicellularity: The Biology of *Escherichia coli* Building
488 Large-Scale Biofilm Communities. Annu Rev Microbiol. 2021;75:269-90. Epub 2021/08/04.
489 doi: 10.1146/annurev-micro-031921-055801. PubMed PMID: 34343018.
490 19. Simm R, Ahmad I, Rhen M, Le Guyon S, Romling U. Regulation of biofilm formation in
491 *Salmonella enterica* serovar Typhimurium. Future Microbiol. 2014;9(11):1261-82. Epub
492 2014/12/02. doi: 10.2217/fmb.14.88. PubMed PMID: 25437188.

493 20. Brown PK, Dozois CM, Nickerson CA, Zuppardo A, Terlonge J, Curtiss R. MIrA, a novel
494 regulator of curli (AgF) and extracellular matrix synthesis by *Escherichia coli* and *Salmonella*
495 *enterica* serovar Typhimurium. Molecular Microbiology. 2001. doi: 10.1046/j.1365-
496 2958.2001.02529.x.
497 21. Ogasawara H, Yamada K, Kori A, Yamamoto K, Ishihama A. Regulation of the
498 *Escherichia coli* csgD promoter: Interplay between five transcription factors. Microbiology.
499 2010. doi: 10.1099/mic.0.039131-0.
500 22. Lindenberg S, Klauck G, Pesavento C, Klauck E, Hengge R. The EAL domain protein YciR
501 acts as a trigger enzyme in a c-di-GMP signalling cascade in *E. coli* biofilm control. EMBO J.
502 2013;32(14):2001-14. Epub 2013/05/28. doi: 10.1038/emboj.2013.120. PubMed PMID:
503 23708798; PubMed Central PMCID: PMCPMC3715855.
504 23. Hengge R. Linking bacterial growth, survival, and multicellularity - small signaling
505 molecules as triggers and drivers. Curr Opin Microbiol. 2020;55:57-66. Epub 2020/04/04. doi:
506 10.1016/j.mib.2020.02.007. PubMed PMID: 32244175.
507 24. Sarenko O, Klauck G, Wilke FM, Pfiffer V, Richter AM, Herbst S, et al. More than
508 Enzymes That Make or Break Cyclic Di-GMP-Local Signaling in the Interactome of GGDEF/EAL
509 Domain Proteins of *Escherichia coli*. mBio. 2017;8(5). Epub 2017/10/12. doi:
510 10.1128/mBio.01639-17. PubMed PMID: 29018125; PubMed Central PMCID:
511 PMCPMC5635695.
512 25. DePas WH, Hufnagel DA, Lee JS, Blanco LP, Bernstein HC, Fisher ST, et al. Iron induces
513 bimodal population development by *Escherichia coli*. Proc Natl Acad Sci U S A.
514 2013;110(7):2629-34. Epub 2013/01/30. doi: 10.1073/pnas.1218703110. PubMed PMID:
515 23359678; PubMed Central PMCID: PMCPMC3574911.
516 26. Serra DO, Richter AM, Klauck G, Mika F, Hengge R. Microanatomy at cellular resolution
517 and spatial order of physiological differentiation in a bacterial biofilm. mBio.
518 2013;4(2):e00103-13. Epub 2013/03/21. doi: 10.1128/mBio.00103-13. PubMed PMID:
519 23512962; PubMed Central PMCID: PMCPMC3604763.
520 27. Serra DO, Hengge R. A c-di-GMP-Based Switch Controls Local Heterogeneity of
521 Extracellular Matrix Synthesis which Is Crucial for Integrity and Morphogenesis of *Escherichia*
522 *coli* Macrocolony Biofilms. J Mol Biol. 2019;431(23):4775-93. Epub 2019/04/08. doi:
523 10.1016/j.jmb.2019.04.001. PubMed PMID: 30954572.
524 28. Besharova O, Suchanek VM, Hartmann R, Drescher K, Sourjik V. Diversification of gene
525 expression during formation of static submerged biofilms by *Escherichia coli*. Frontiers in
526 Microbiology. 2016. doi: 10.3389/fmicb.2016.01568.
527 29. Grantcharova N, Peters V, Monteiro C, Zakikhany K, Römling U. Bistable expression of
528 CsgD in biofilm development of *Salmonella enterica* serovar Typhimurium. Journal of
529 Bacteriology. 2010. doi: 10.1128/JB.01826-08.
530 30. MacKenzie KD, Wang Y, Shivak DJ, Wong CS, Hoffman LJ, Lam S, et al. Bistable
531 expression of CsgD in *Salmonella enterica* serovar Typhimurium connects virulence to
532 persistence. Infect Immun. 2015;83(6):2312-26. Epub 2015/04/01. doi: 10.1128/IAI.00137-15.
533 PubMed PMID: 25824832; PubMed Central PMCID: PMCPMC4432751.
534 31. Yousef KP, Streck A, Schütte C, Siebert H, Hengge R, von Kleist M. Logical-continuous
535 modelling of post-translationally regulated bistability of curli fiber expression in *Escherichia*
536 *coli*. BMC Systems Biology. 2015. doi: 10.1186/s12918-015-0183-x.
537 32. Baba T, Ara T, Hasegawa M, Takai Y, Okumura Y, Baba M, et al. Construction of
538 *Escherichia coli* K-12 in-frame, single-gene knockout mutants: the Keio collection. Mol Syst

539 Biol. 2006;2:2006 0008. Epub 2006/06/02. doi: 10.1038/msb4100050. PubMed PMID:
540 16738554; PubMed Central PMCID: PMCPMC1681482.
541 33. Cherepanov PP, Wackernagel W. Gene disruption in *Escherichia coli*: TcR and KmR
542 cassettes with the option of Flp-catalyzed excision of the antibiotic-resistance determinant.
543 Gene. 1995;158(1):9-14. Epub 1995/05/26. doi: 10.1016/0378-1119(95)00193-a. PubMed
544 PMID: 7789817.
545 34. Amann E, Ochs B, Abel K-J. Tightly regulated tac promoter vectors useful for the
546 expression of unfused and fused proteins in *Escherichia coli*. Gene. 1988;69(2):301-15. doi:
547 https://doi.org/10.1016/0378-1119(88)90440-4.
548 35. Wang P, Robert L, Pelletier J, Dang WL, Taddei F, Wright A, et al. Robust growth of
549 *Escherichia coli*. Curr Biol. 2010;20(12):1099-103. Epub 2010/06/12. doi:
550 10.1016/j.cub.2010.04.045. PubMed PMID: 20537537; PubMed Central PMCID:
551 PMCPMC2902570.
552 36. Potrykus K, Cashel M. (p)ppGpp: still magical? Annu Rev Microbiol. 2008;62:35-51.
553 Epub 2008/05/06. doi: 10.1146/annurev.micro.62.081307.162903. PubMed PMID: 18454629.
554 37. Varik V, Oliveira SRA, Hauryliuk V, Tenson T. HPLC-based quantification of bacterial
555 housekeeping nucleotides and alarmone messengers ppGpp and pppGpp. Sci Rep.
556 2017;7(1):11022. Epub 2017/09/10. doi: 10.1038/s41598-017-10988-6. PubMed PMID:
557 28887466; PubMed Central PMCID: PMCPMC5591245.
558 38. Patacq C, Chaudet N, Letisse F. Crucial Role of ppGpp in the Resilience of *Escherichia*
559 *coli* to Growth Disruption. mSphere. 2020;5(6). Epub 2020/12/29. doi:
560 10.1128/mSphere.01132-20. PubMed PMID: 33361126; PubMed Central PMCID:
561 PMCPMC7763551.
562 39. Krasteva PV, Fong JC, Shikuma NJ, Beyhan S, Navarro MV, Yildiz FH, et al. *Vibrio*
563 *cholerae* VpsT regulates matrix production and motility by directly sensing cyclic di-GMP.
564 Science. 2010;327(5967):866-8. Epub 2010/02/13. doi: 10.1126/science.1181185. PubMed
565 PMID: 20150502; PubMed Central PMCID: PMCPMC2828054.
566 40. Ahmad I, Cimdins A, Beske T, Romling U. Detailed analysis of c-di-GMP mediated
567 regulation of csgD expression in *Salmonella typhimurium*. BMC Microbiol. 2017;17(1):27. Epub
568 2017/02/06. doi: 10.1186/s12866-017-0934-5. PubMed PMID: 28148244; PubMed Central
569 PMCID: PMCPMC5289004.
570 41. Gualdi L, Tagliabue L, Landini P. Biofilm formation-gene expression relay system in
571 *Escherichia coli*: modulation of sigmaS-dependent gene expression by the CsgD regulatory
572 protein via sigmaS protein stabilization. J Bacteriol. 2007;189(22):8034-43. Epub 2007/09/18.
573 doi: 10.1128/JB.00900-07. PubMed PMID: 17873038; PubMed Central PMCID:
574 PMCPMC2168689.
575 42. Levine JH, Lin Y, Elowitz MB. Functional roles of pulsing in genetic circuits. Science.
576 2013;342(6163):1193-200. Epub 2013/12/07. doi: 10.1126/science.1239999. PubMed PMID:
577 24311681; PubMed Central PMCID: PMCPMC4100686.
578 43. Locke JC, Young JW, Fontes M, Hernandez Jimenez MJ, Elowitz MB. Stochastic pulse
579 regulation in bacterial stress response. Science. 2011;334(6054):366-9. Epub 2011/10/08. doi:
580 10.1126/science.1208144. PubMed PMID: 21979936; PubMed Central PMCID:
581 PMCPMC4100694.
582 44. Levine JH, Fontes ME, Dworkin J, Elowitz MB. Pulsed feedback defers cellular
583 differentiation. PLoS Biol. 2012;10(1):e1001252. Epub 2012/02/04. doi:
584 10.1371/journal.pbio.1001252. PubMed PMID: 22303282; PubMed Central PMCID:
585 PMCPMC3269414.

586 45. Patange O, Schwall C, Jones M, Villava C, Griffith DA, Phillips A, et al. *Escherichia coli*
587 can survive stress by noisy growth modulation. Nat Commun. 2018;9(1):5333. Epub
588 2018/12/19. doi: 10.1038/s41467-018-07702-z. PubMed PMID: 30559445; PubMed Central
589 PMCID: PMCPMC6297224.
590 46. Kim JM, Garcia-Alcala M, Balleza E, Cluzel P. Stochastic transcriptional pulses
591 orchestrate flagellar biosynthesis in *Escherichia coli*. Sci Adv. 2020;6(6):eaax0947. Epub
592 2020/02/23. doi: 10.1126/sciadv.aax0947. PubMed PMID: 32076637; PubMed Central
593 PMCID: PMCPMC7002133.
594 47. Sassi AS, Garcia-Alcala M, Kim MJ, Cluzel P, Tu Y. Filtering input fluctuations in intensity
595 and in time underlies stochastic transcriptional pulses without feedback. Proc Natl Acad Sci U
596 S A. 2020;117(43):26608-15. Epub 2020/10/14. doi: 10.1073/pnas.2010849117. PubMed
597 PMID: 33046652; PubMed Central PMCID: PMCPMC7604450.
598

599

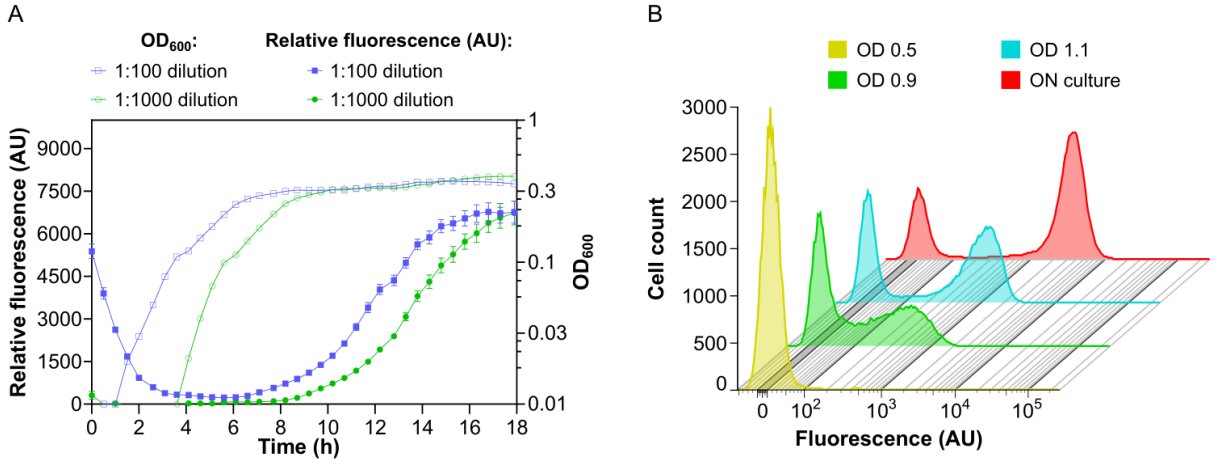

600

601 **Figure 1: Bimodal activation of curli gene expression in *E. coli* planktonic cultures.** *E. coli* cells
602 carrying genomic transcriptional reporter of *csgBAC* operon were grown in liquid tryptone broth (TB)
603 medium at 30 °C under constant shaking. **(A)** Optical density (OD_{600}) and relative fluorescence
604 (fluorescence/OD_{600}; AU, arbitrary units) of the culture during growth in a plate reader, starting from two
605 different dilutions of the overnight culture. Error bars indicate standard error of the mean (SEM) of 10
606 technical replicates. **(B)** Distribution of single-cell fluorescence levels, measured by flow cytometry, of
607 cultures grown from overnight culture diluted 1:1000 to indicated OD_{600} or overnight (ON; 25 h) in flasks
608 in an orbital shaker.

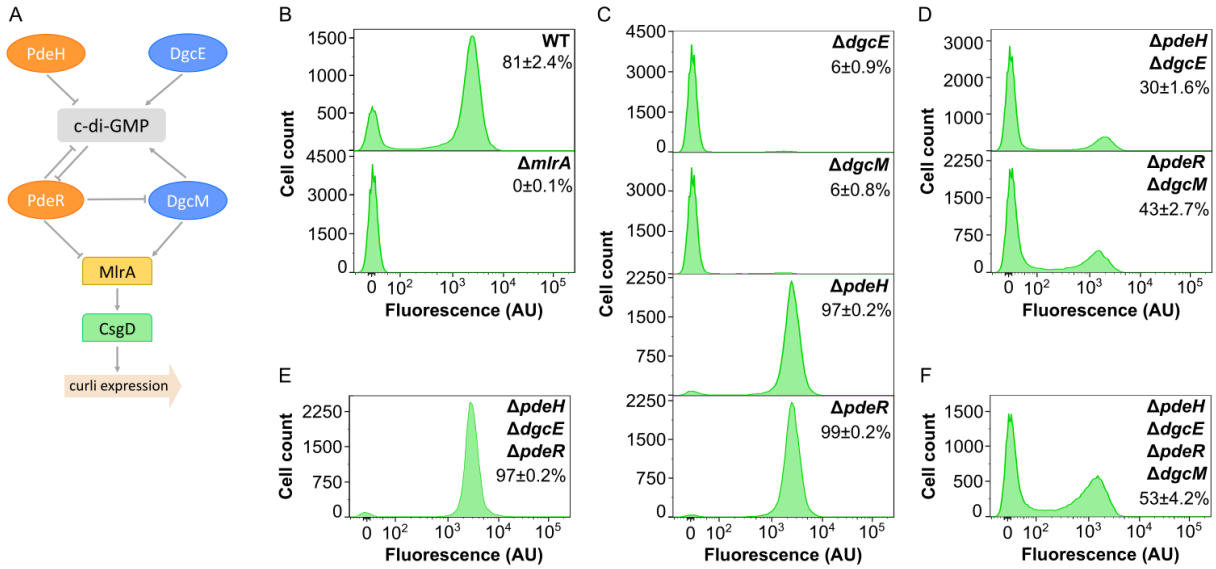

Figure 2: Regulation of curli gene expression by c-di-GMP. (A) Current model of regulation of curli gene expression by c-di-GMP in *E. coli*, adapted from [27]. The regulation is mediated by two pairs of diguanylate cyclases (DGCs; blue) and phosphodiesterases (PDEs; orange). PdeH and DgcE control global levels of c-di-GMP, whereas PdeR and DgcM mediate local c-di-GMP-dependent regulation of curli gene expression by controlling activity of transcription factor MlrA, which activates another curli-specific transcription factor CsgD. **(B-F)** Flow cytometry measurements of curli gene expression in *E. coli* planktonic cultures grown in TB overnight in flasks in an orbital shaker, shown for the wild-type (WT) and Δ*mlrA* strain (B), and individual (C), double (D), triple (E) and quadruple (F) deletions of DGC or PDE enzymes, as indicated. Fraction of positive cells in the population (mean of three biological replicates ± SEM) is indicated for each strain. Note that the scale in the *y* axes is different for individual strains to improve readability.

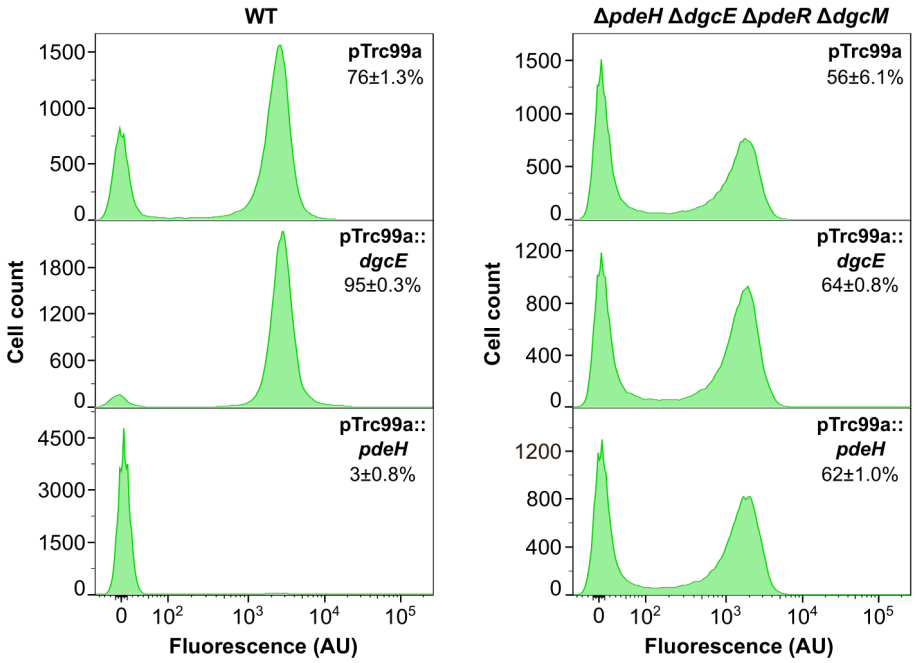

Figure 3: Decoupling of curli gene expression from c-di-GMP regulation in the absence of PdeR/ DgcM regulatory module. *E. coli* wild-type (WT) cells or cells lacking c-di-GMP regulatory enzymes (Δ*pdeH* Δ*dgcE* Δ*pdeR* Δ*dgcM*) were transformed with either empty pTrc99a plasmid (control) or with pTrc99a plasmid carrying *dgcE* (pTrc99a::dgcE) or *pdeH* (pTrc99a::pdeH) genes. Expression from the vector was induced with 1 μM IPTG. Bacteria were grown in TB overnight in flasks with shaking and cultures were subjected to the flow cytometry analysis. Fraction of positive cells in the population (mean of three biological replicates ± SEM) is indicated for each strain.

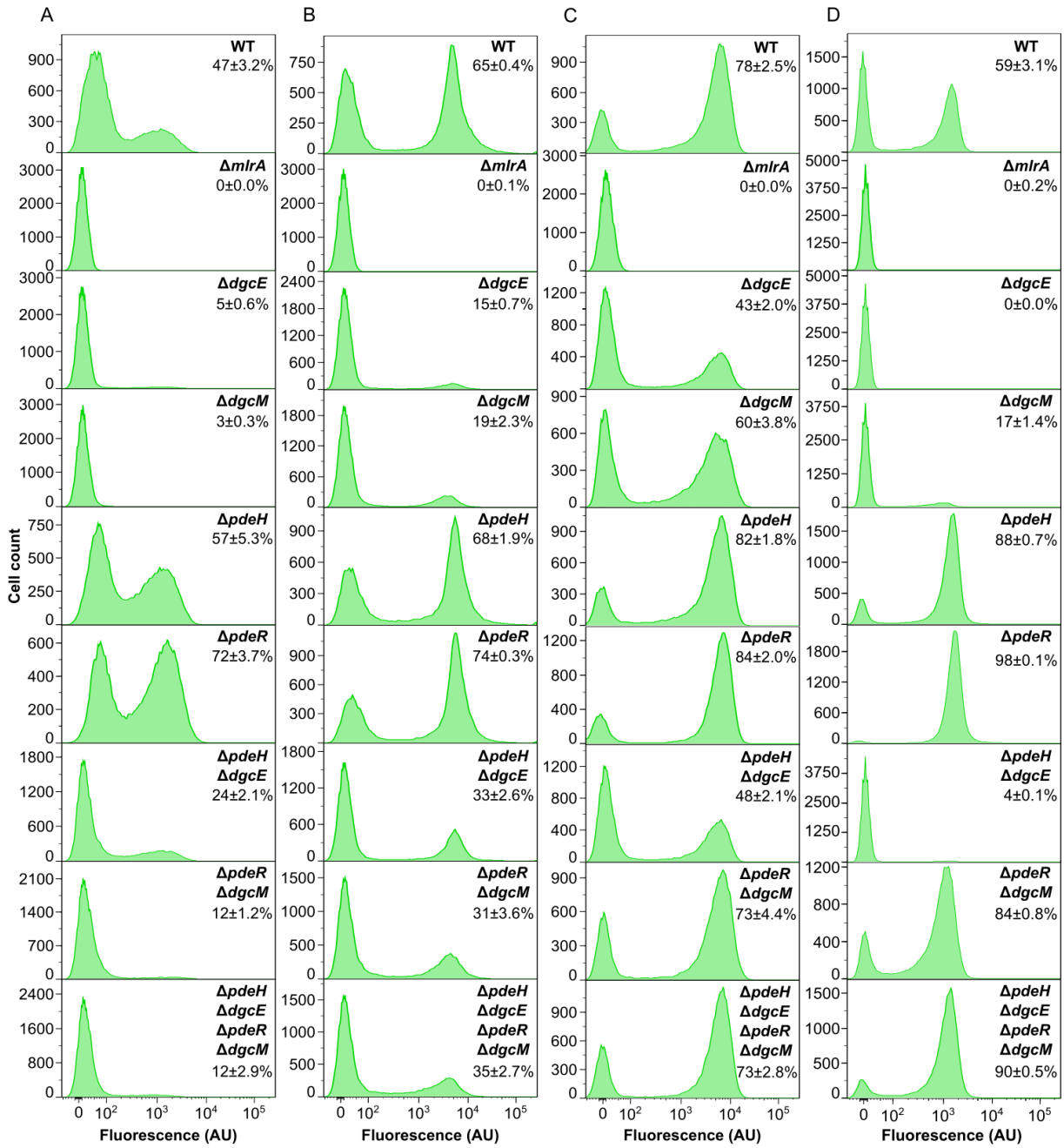

Figure 4: Dependence of curli gene expression on c-di-GMP regulation under different growth conditions. (A-D) Flow cytometry measurements of curli expression in the wildtype (WT) and indicated gene deletion strains either after 24 h of growth in liquid TB in a plate reader (A) or as submerged biofilms without agitation (B), as macrocolony biofilms on salt-free LB agar (C), or as overnight planktonic cultures in salt-free LB in flasks in an orbital shaker. Fraction of positive cells in the population (mean of three biological replicates ± SEM) is indicated for each strain.

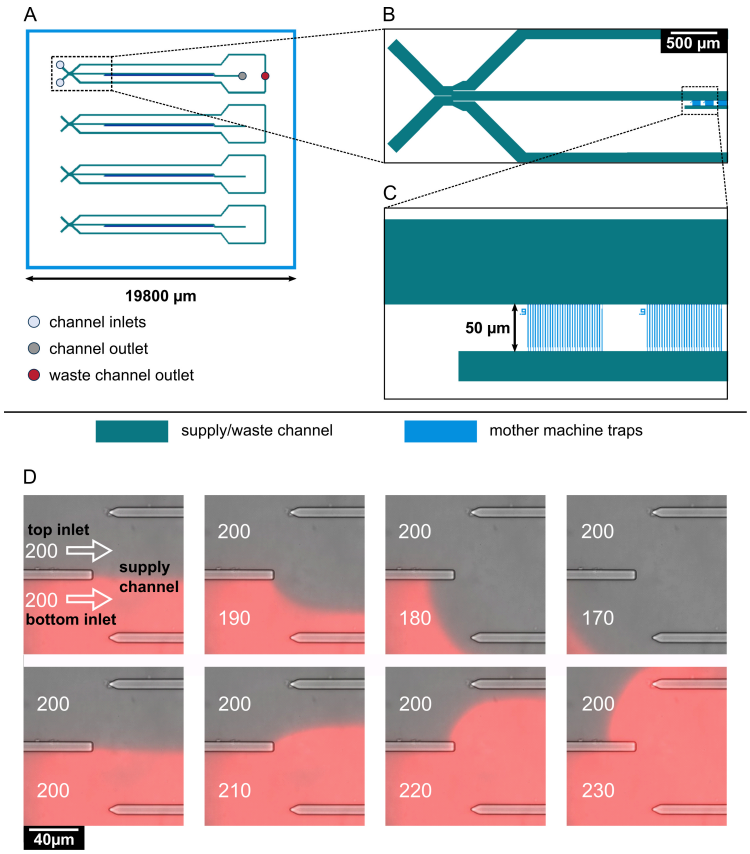

Figure 5: Design and operation of the microfluidic mother machine device. (A) Schematic overview of the chip layout, featuring four independent supply channels (green) for cell inoculation and media supply. **(B)** Detailed view of the area marked by a rectangle in (A), showing the switching junction and a part of the mother machine cultivation sites (blue). The junction is formed by two inlets, leading to one central supply channel. Control of pressure at each inlet allows for prioritization of one medium over the other through the supply channel, and, ultimately, the mother machine cultivation sites. Residual medium flows out through waste channels located to each side of the central supply channel. Medium flowing through the supply channel exits the chip through one outlet. **(C)** Detailed view of the area marked in **(B)** by a rectangle, showing the mother machine cultivation sites. Each of the four channels contains 57 mother machine cultivation sites, each of which contains 30 mother machine traps with widths of either 0.9, 1, or 1.1 µm. The mother machine traps feature a 0.3 µm wide constriction on the bottom, preventing the mother cell from exiting the trap while allowing perfusion of the medium. The supply channels (green) are 8 µm in depth, the mother machine traps (blue) are 0.8 µm in depth. **(D)** On-chip medium switching visualized by merged phase contrast and mCherry images of the channel junction. Media are supplied through separate inlets (top and bottom), which are separated in the center of the channel by a PDMS barrier. The direction of flow is indicated by white arrows. Water was supplied through the top inlet, while a 0.2 µM sulforhodamine B solution was supplied through the bottom inlet, visualizing the flow pattern in the junction. The pressure at the top inlet was kept constant at 200 mbar. Depending on the pressure set at the bottom inlet, it is possible to select which one of the two media flows into the central supply channel to the mother machine growth sites.

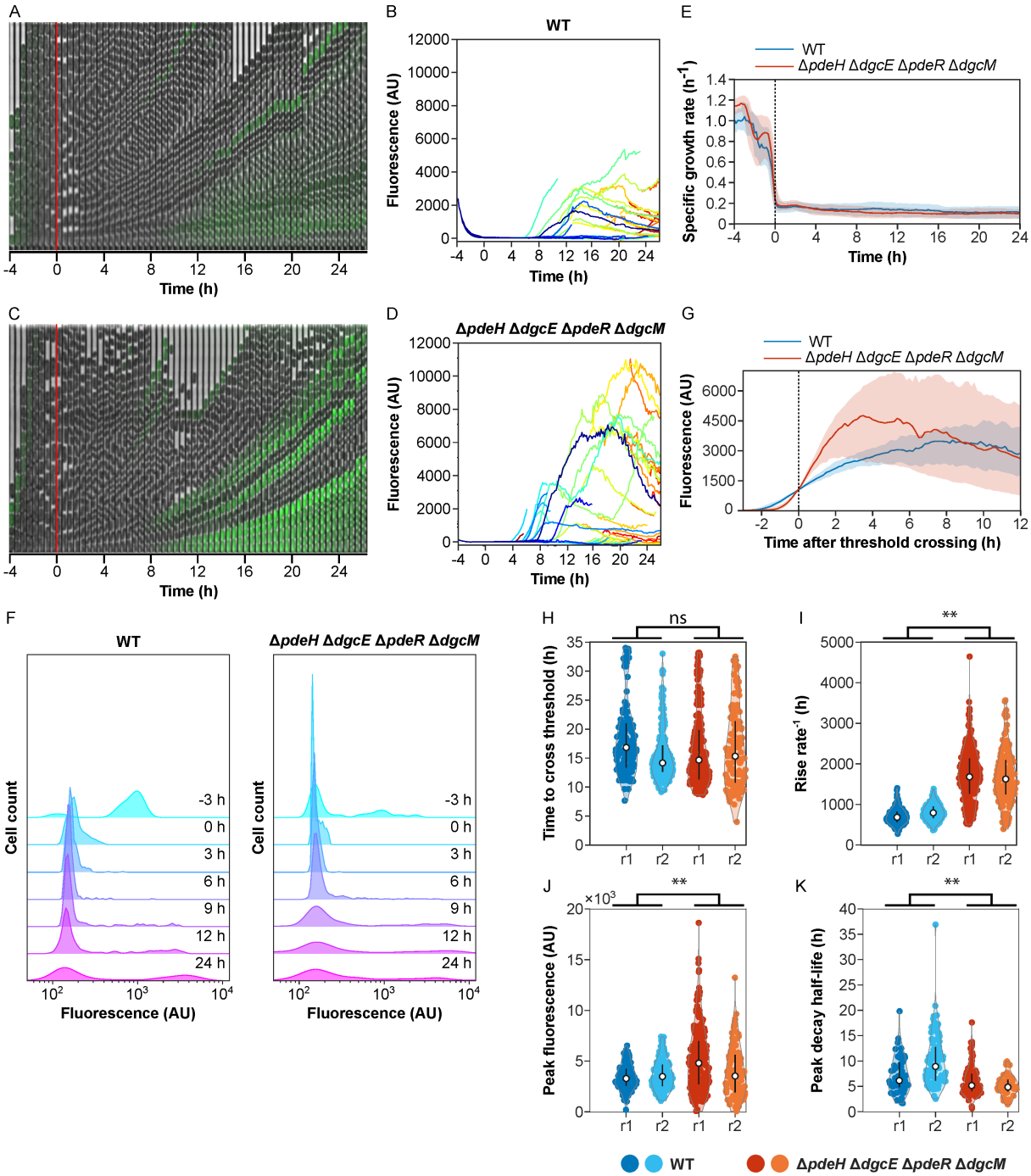

Figure 6: Impact of c-di-GMP regulation on dynamics of curli gene induction in individual cells. *E. coli* cells in a microfluidic device (mother machine) were shifted from a fresh to conditioned TB medium after 4 h of growth to induce curli expression. **(A-D)** Examples of image time series and single-cell fluorescence traces for the wild-type (WT) (A,B) and for the Δ*pdeH* Δ*dgcE* Δ*pdeR* Δ*dgcM* strain disabled in the c-di-GMP regulation (C,D), growing in a mother machine in one experiment. Expression of the curli reporter is indicated by the green overlay on the phase contrast image. **(E)** Median instantaneous growth rate — fold rate of change in length — of cells grown in microfluidics experiments as described in (A). The switch to conditioned medium is at time zero, as indicated. Shaded area is the interquartile range. The number of cells in the device varies with time, but is on average n = 296 for WT and n = 522 for the quadruple deletion strain. **(F)** Distributions of curli expression at different time points

670 in the microfluidics experiment. Shown are kernel density estimates of curli expression in WT and in the
671 quadruple deletion strain at selected time points. **(G)** Median curli expression profile for single-cell traces
672 aligned by the time at which they exceed a threshold of 10^3 fluorescence units. Shaded area is
673 interquartile range; n = 128 for WT and 230 for the quadruple deletion strain. **(H-K)** Distributions of curli
674 induction parameters for the wild-type and for the c-di-GMP-regulation disabled strain, in two
675 independent experiments, r1 (same experiment as in A-G) and r2. Shown are histograms of the times
676 at which a threshold of 10^3 fluorescence units were crossed **(H)**, the maximum rates of increase in
677 fluorescence **(I)**, the fluorescence amplitudes at the first peak **(J)** and the half-time of fluorescence decay
678 after reaching the peak **(K)** for cell traces from both microfluidics experiments. $^{**}p<10^{-2}$ in an unpaired
679 two-sample *t*-test assuming normal distributions with unknown and unequal variances. ns, non-
680 significant.

681

682 ## Supporting information

683

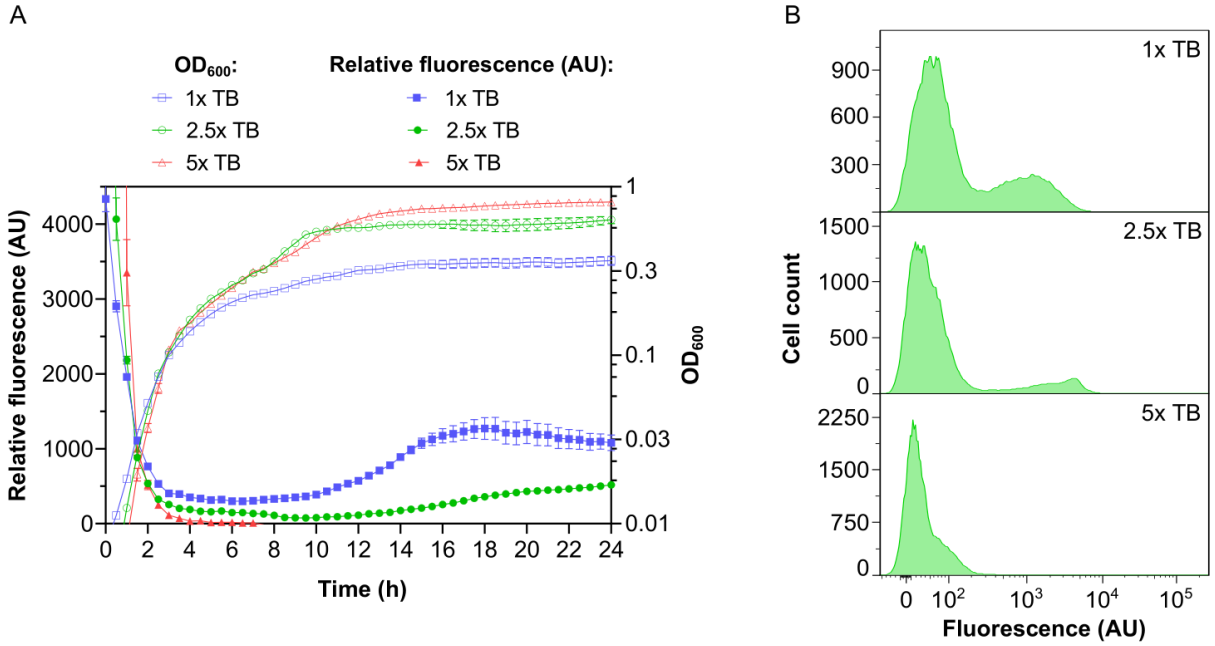

684

685 **Figure S1: Dependence of curli gene expression on nutrient levels.** Wild-type *E. coli* cultures were
686 grown as in Figure 1A but with different indicated concentrations of TB. **(A)** Bacterial growth and activity
687 of transcriptional curli reporter. Error bars indicate SEM of 6 technical replicates. **(B)** Distribution of
688 single-cell fluorescence levels after 24 h of growth in a plate reader measured by flow cytometry. Note
689 that the scale in the *y* axes is different for individual conditions to improve readability.

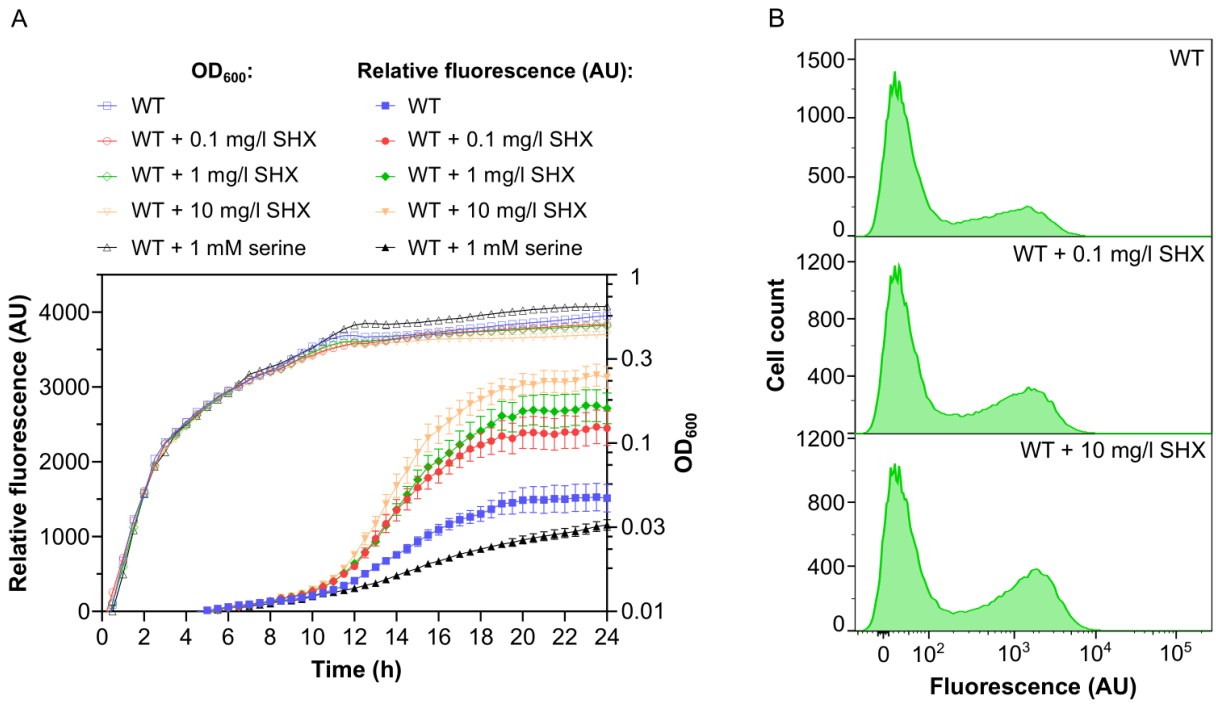

Figure S2: Stimulation of curli gene expression by stringent response. Wild-type *E. coli* cultures were grown as in Figure 1A but with addition of either indicated concentrations of serine hydroxamate (SHX) at inoculation point or 1 mM serine after 6 h of growth. **(A)** Bacterial growth and activity of transcriptional curli reporter. Error bars indicate SEM of 6 technical replicates. **(B)** Distribution of single-cell fluorescence levels after 24 h of growth in a plate reader measured by flow cytometry.

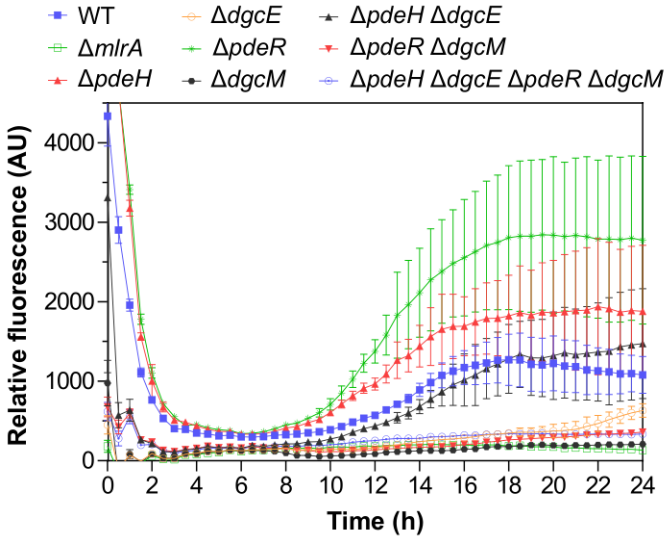

Figure S3: Relative fluorescence of curli reporter in planktonic culture grown in TB medium in a plate reader. Error bars indicate SEM of 5 technical replicates. *E. coli* planktonic cultures of the wild-type (WT), Δ*mlrA* strain, and individual, double and quadruple deletions of DGC or PDE enzymes were grown in TB in a plate reader.

701

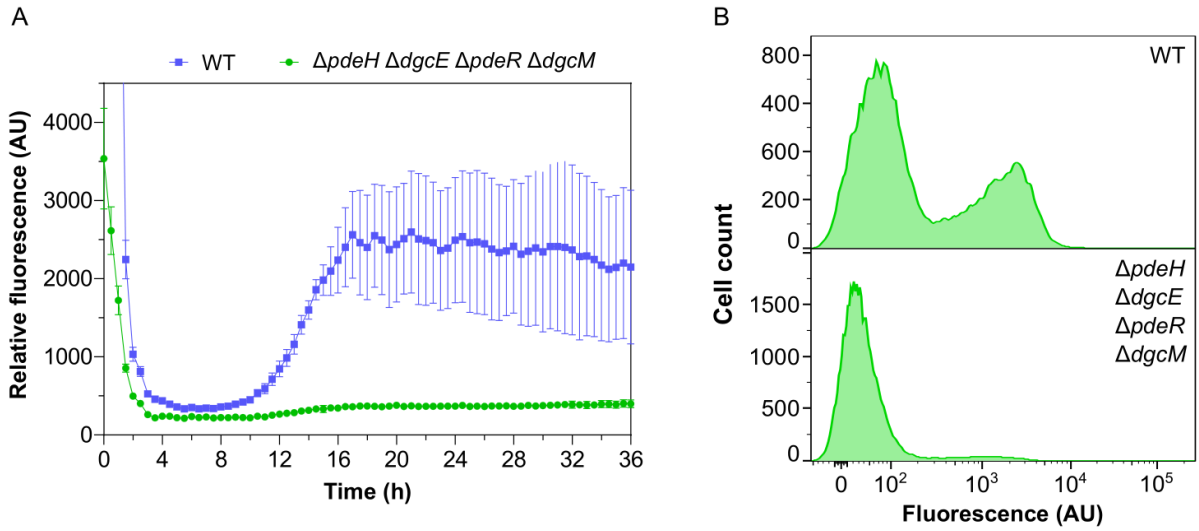

702

703 **Figure S4: Curli gene expression upon prolonged cultivation in a plate reader.** Wild-type (WT) and
704 Δ*pdeH* Δ*dgcE* Δ*pdeR* Δ*dgcM* strains were grown in TB in a plate reader as in Figure S3, but during
705 36 h. **(A)** Induction of transcriptional curli reporter. Error bars indicate SEM of 10 technical replicates.
706 **(B)** Distribution of single-cell fluorescence levels in populations of both strains after 36 h of growth
707 measured by flow cytometry.

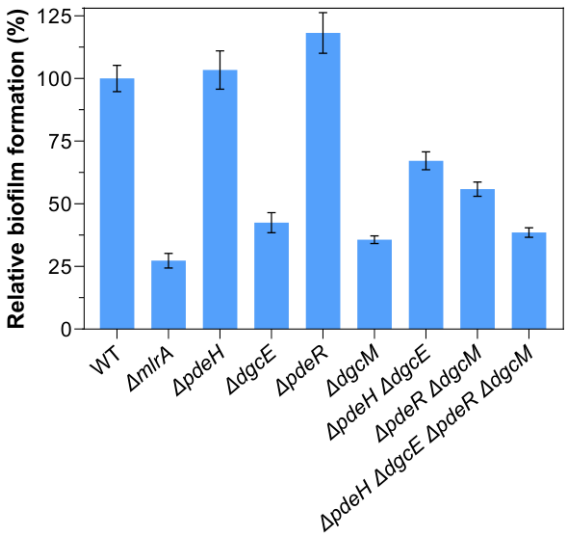

708

709 **Figure S5: Curli gene expression in submerged biofilm cultures.** Biofilm formation by indicated
710 strains grown in multi-well plates in TB medium, quantified using crystal violet (CV) staining. Error bars
711 indicate SEM of 3 independent replicates.

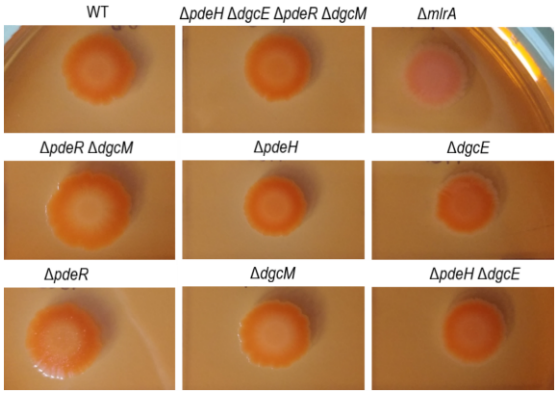

Figure S6: Curli expression in macrocolony biofilms. Images of macrocolonies of indicated strains after 8 days of growth on salt-free LB agar plates.

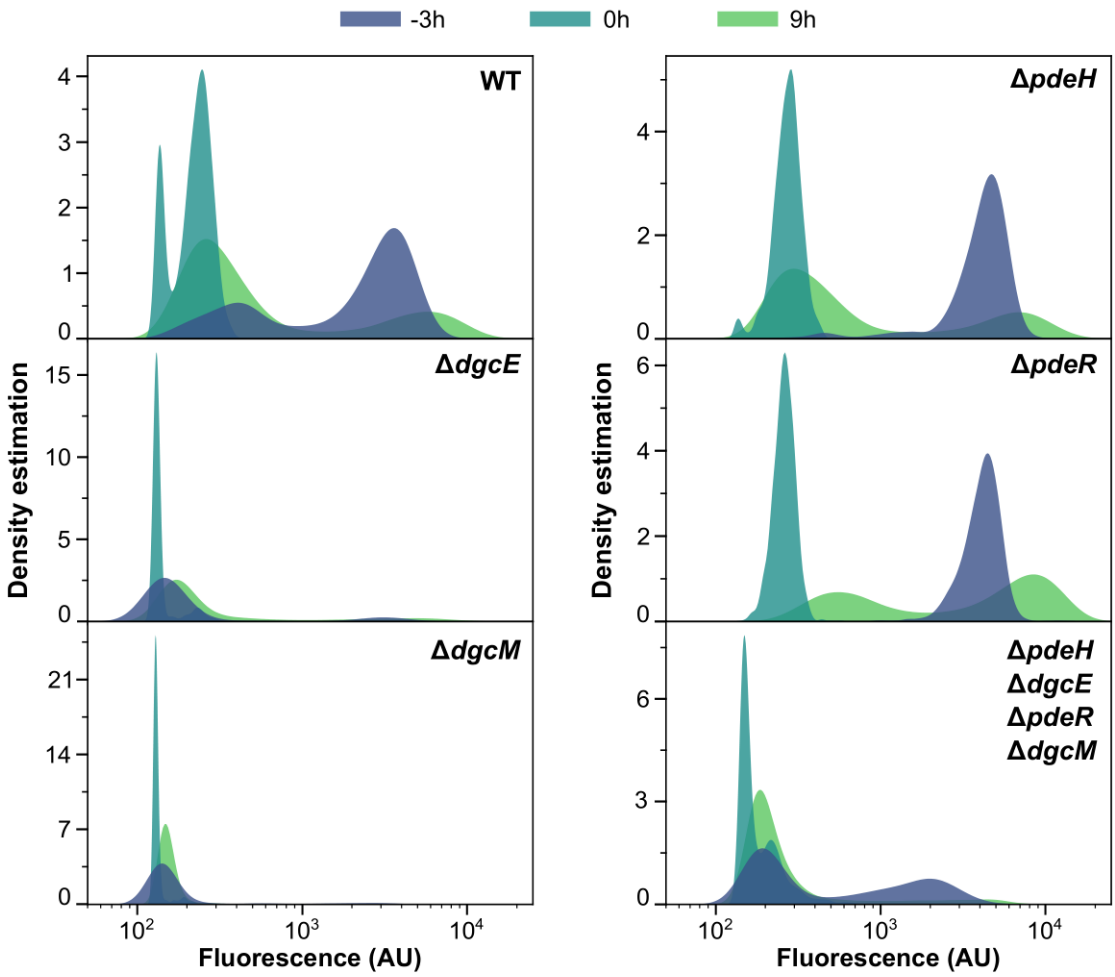

Figure S7: Distributions of curli expression at different time points in the microfluidics experiment. Shown are kernel density estimates of curli expression in the wild type WT, individual and quadruple deletions of DGC or PDE enzymes at selected time points. Cells in stationary phase were loaded into mother machine chip supplied with fresh medium, and then switched to the conditioned media at the ''0 hours'' time point. Note that the scale in the *y* axes is different for individual conditions to improve readability.

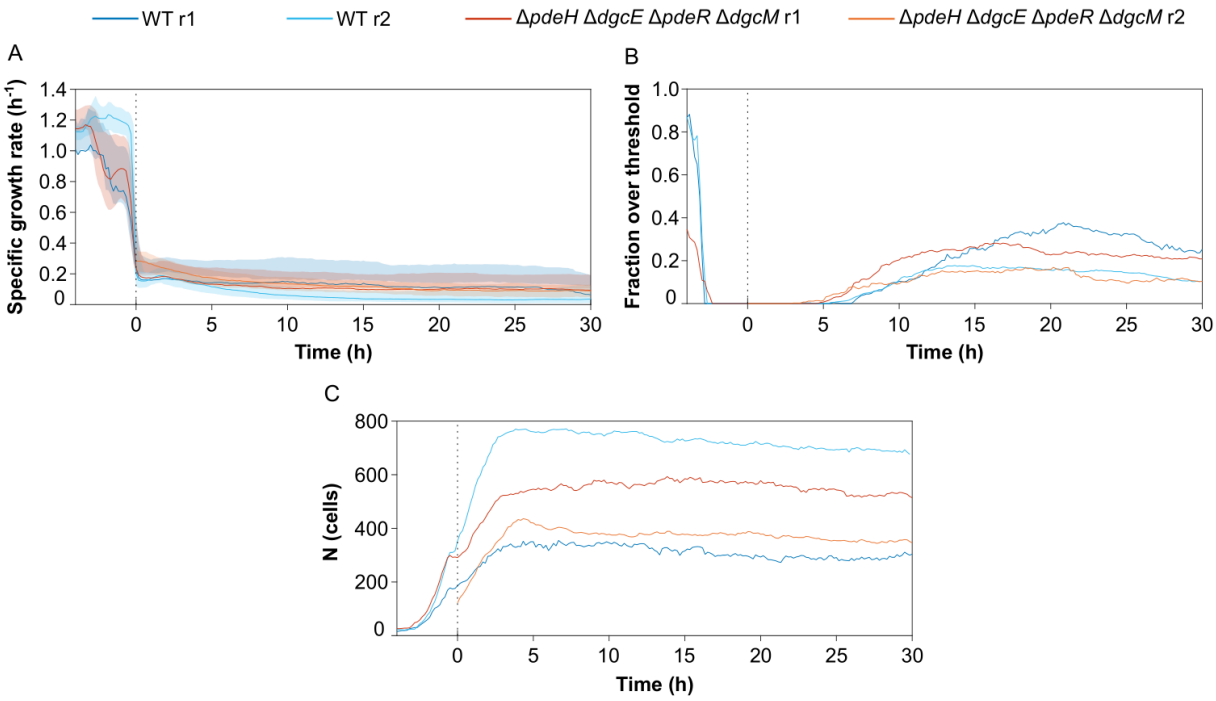

Figure S8: Growth rates and fraction of curli expressing cells over time. Stationary phase cells were introduced into mother machine devices, supplied with fresh medium and then switched to conditioned medium after 4 h of growth, as in Figure 6. **(A)** Median instantaneous growth rates for the wild-type and for the Δ*pdeH* Δ*dgcE* Δ*pdeR* Δ*dgcM* strain disabled in c-di-GMP regulation. Growth rate drops rapidly and cells switch on curli expression after a switch to conditioned medium. Shaded area is interquartile range. **(B)** Fraction of cells with fluorescence exceeding 1000 units. **(C)** Number of detected cells. Two biological replicates (r1 and r2) were performed for each strain; data for the r1 replicate are also shown in Figure 6. Note that in the r2 experiment for the quadruple deletion strain, cells were only imaged after medium switching.

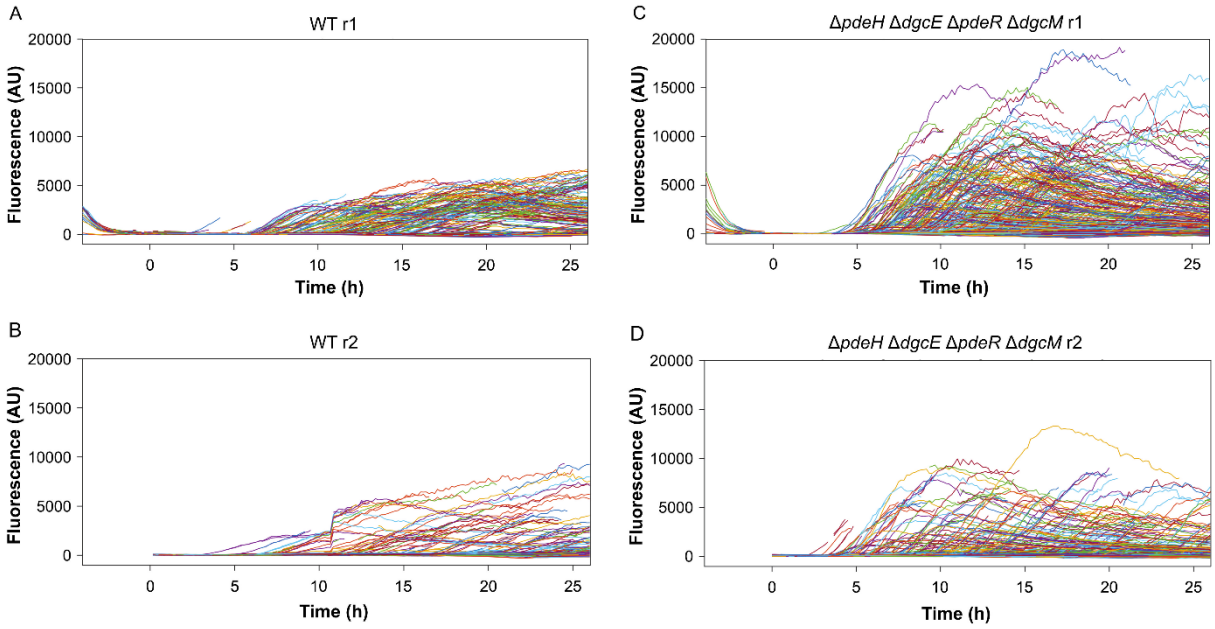

732

733 **Figure S9: Single-cell traces of cell fluorescence for all cells for the wild-type and for the c-di-**
734 **GMP-regulation disabled strain.** Data are from the same biological replicates (r1 and r2) as in Figure
735 S8.

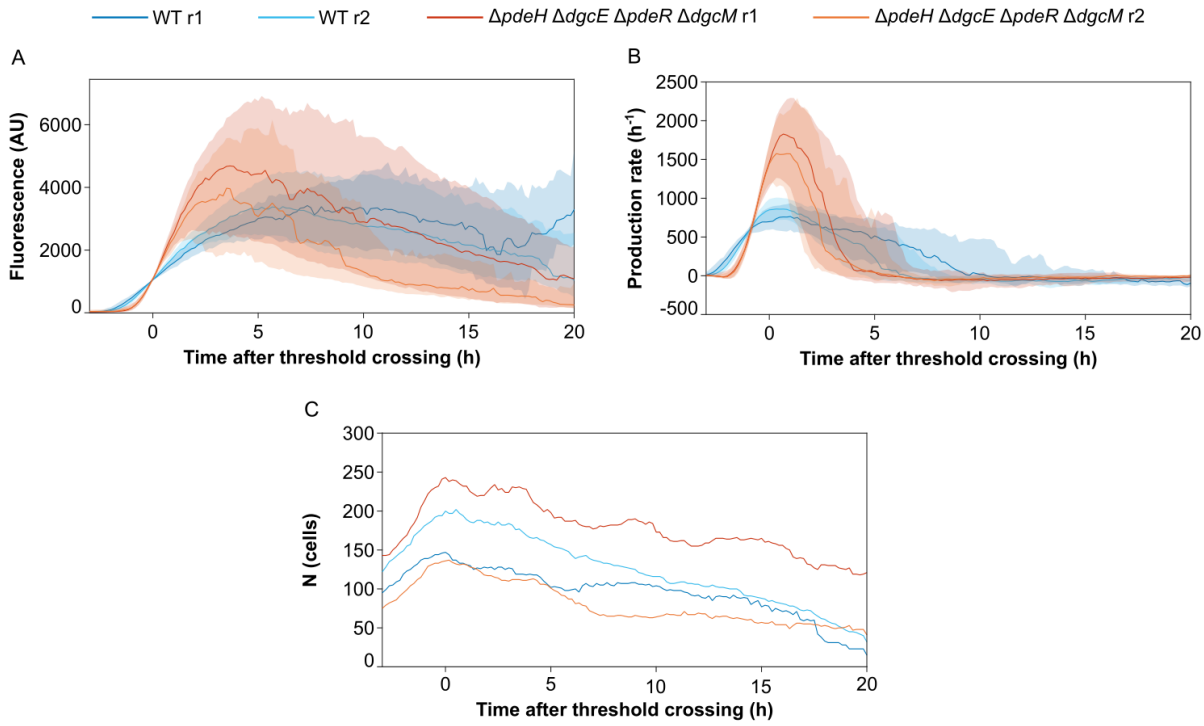

Figure S10: The rate and variability of curli induction for the wild-type and for the c-di-GMP-regulation disabled strain. (A) Median curli expression, **(B)** production rate, and **(C)** number of cells for traces from both microfluidics experiments (r1 and r2) aligned by the time at which they exceeded a threshold of 10^3 fluorescence units. Shaded area is interquartile range. Compared to the WT, the rate of curli induction is faster but traces show more variability in a mutant without the global or local c-di-GMP regulatory modules.

744 **Table S1. *E. coli* strains and plasmids used in this study.**

Strains	Relevant genotype	Reference
W3110	W3110 derivative with functional RpoS	[1]
VS1146	W3110 *csgA*::*csgA*_RBS_*sfgfp*	[2]
VS1857	VS1146 Δ*mlrA*	This work
VS1732	VS1146 Δ*pdeH*	This work
VS1720	VS1146 Δ*dgcE*	This work
VS1258	VS1146 Δ*pdeR*	This work
VS1257	VS1146 Δ*dgcM*	This work
VS1717	VS1146 Δ*pdeH* Δ*dgcE*	This work
VS1713	VS1146 Δ*pdeR* Δ*dgcM*	This work
VS1885	VS1146 Δ*pdeH* Δ*dgcE* Δ*pdeR*	This work
VS1729	VS1146 Δ*pdeH* Δ*dgcE* Δ*pdeR* Δ*dgcM*	This work
Plasmids		
pTrc99a	Expression vector; *Ptrc* promoter inducible by isopropyl-β-D-thiogalactopyranoside (IPTG); pBR ori; Ap^R	[3]
pVS2689	pTrc99a::*pdeH*	This work
pVS1644	pTrc99a::*dgcE*	This work

745

746 1. Serra DO, Richter AM, Klauck G, Mika F, Hengge R. Microanatomy at cellular resolution and
747 spatial order of physiological differentiation in a bacterial biofilm. mBio. 2013;4(2):e00103-13. Epub
748 2013/03/21. doi: 10.1128/mBio.00103-13. PubMed PMID: 23512962; PubMed Central PMCID:
749 PMCPMC3604763.
750 2. Besharova O, Suchanek VM, Hartmann R, Drescher K, Sourjik V. Diversification of gene
751 expression during formation of static submerged biofilms by *Escherichia coli*. Frontiers in Microbiology.
752 2016. doi: 10.3389/fmicb.2016.01568.
753 3. Amann E, Ochs B, Abel K-J. Tightly regulated tac promoter vectors useful for the expression of
754 unfused and fused proteins in *Escherichia coli*. Gene. 1988;69(2):301-15. doi:
755 https://doi.org/10.1016/0378-1119(88)90440-4.

756

Supporting protocols

Design and fabrication of the mother machine. A microfluidic device was used for time-resolved studies of *E. coli* growth and curli expression, which features mother machines traps for the observation of one-dimensional cell growth. The design of the microfluidic device is shown in Figure 5. The channel structure of the microfluidic chip features four independent channels with a depth of 8 µm, allowing the realization of four conditions, e.g. different media compositions, in one experiment. Each channel contains two inlets enabling on-chip switching between two different media, which are supplied at defined pressures. By controlling the pressure ratio between the two inlets, the medium supplied at the higher pressure flows through the central channel following the junction, while the other medium is pushed away from the junction and flows out through the waste channel (Figure 5D). The medium which flows through the central channel reaches the mother machine cultivation sites before exiting the chip through a single outlet.

The device was produced using a two-layer soft lithography method as described previously [1]. Based on our in-house made design of the channel layout, a 100 mm silicon wafer was produced by e-beam lithography (ConScience, Sweden). The wafer contains the channel layout as a positive relief. The mother machine traps, which are shown in blue in Figure 5A-C, were structured by etching the wafer by 0.8 µm, giving the mother machine the appropriate vertical dimension for cell trapping. The supply channels, which are shown in green in Figure 5A-C, are implemented as photoresist structures with a height of 8 µm on the wafer. The wafer served as a master mold for liquid polydimethylsiloxane (Sylgard 184 PDMS, VwR International GmbH, Germany), which was mixed at volumetric ratio of 7:1 with a cross-linking agent, degassed in a desiccator for 30 min and poured over the wafer to a height of approximately 4 mm and thermally cured at 80 °C overnight. The cured PDMS was peeled off from the wafer and manually cut into separate chips. Inlet and outlet holes were punched with a 0.75 mm punching tool (Robbins True-Cut Disposable Biopsy Punch 0.75mm with Plunger, Robbins Instruments, USA). The surface of the chip was cleaned by a rinse with isopropanol and the application of adhesive tape (tesafilm, Germany) prior to bonding. The chip was irreversibly bonded to a glass substrate by applying oxygen plasma to both chip and glass surfaces (Diener Femto, Diener GmbH, Germany) and bringing the treated surfaces together. The bond was strengthened by storing the bonded device in the oven at 80 °C for 2 min. The device was mounted on an inverted fluorescence microscope (Nikon Eclipse Ti, Nikon Corporation, Japan) equipped with an incubator. The microscope setup included an Andor Zyla 4.2 sCMOS camera (Oxford Instruments, UK), an objective with 100x magnification (Plan Apochromat λ Oil, NA=1.45, WD=170 µm; Nikon, Japan) and a perfect focus system (Nikon Corporation, Japan) for focus drift compensation.

794

795 **Growth experiments.** *E. coli* cells were allowed to grow in TB medium until the stationary
796 phase prior to inoculation into the device. Conditioned medium was prepared by cultivating the
797 wild-type *E. coli* cells in TB medium for 20 h (batch culture), after which the cell suspension
798 was centrifuged at 4000 rpm for 10 min. The medium then was filter sterilized and stored at
799 4°C. The mother machine growth sites were loaded with the undiluted cell suspension by
800 manual infusion of the cell suspension through one of the two inlets using a 1-ml syringe. The
801 connection between the syringe and the chip was realized by tygon tubing (Tygon S-54-HL,
802 inner diameter = 0.51 mm, outer diameter = 1.52 mm, VwR International GmbH, Germany) in
803 combination with blunt dispensing needles (general purpose tips, inner diameter = 0.41 mm,
804 outer diameter = 0.72 mm, Nordson EFD, USA). Medium flow was controlled by programmable
805 pressure regulators (LineUP FlowEZ, FLUIGENT, France), which generated flow by applying
806 pressure on 50-ml medium reservoirs (P-CAP series, FLUIGENT, France). Fresh and
807 conditioned TB medium were respectively filled in separate reservoirs, and each one was
808 pressurized by one module of the pressure regulator. After the cell inoculation both media were
809 connected to the inlets of the channel via tygon tubing and blunt dispensing needles. The
810 pressure at the inlet of the fresh TB medium was set to 200 mbar and remained constant
811 throughout the experiment. During the selection of the positions for imaging the pressure at
812 the inlet of the conditioned medium was set to 250 mbar, allowing the conditioned medium to
813 flow through the junction to the mother machine growth sites and thereby maintaining the
814 stationary state of the cells. At the beginning of imaging, the pressure at the inlet of the
815 conditioned medium was reduced to 150 mbar and programmed to increase back to 250 mbar
816 after 4 h of on-chip cultivation, thereby activating a medium switch from fresh to conditioned
817 TB medium. Phase contrast and GFP fluorescence images were acquired with a time interval
818 of 10 min.

819

820 **Analysis of microfluidics data.** Cells were segmented from phase contrast images by
821 making use of a fully convolutional neural network based on the U-net architecture [2]. A set
822 of manually curated cell outlines was prepared for training (1105 outlines) and validation (346
823 outlines) of the network. The training set was augmented by scaling, rotation, flipping and
824 addition of white noise. A U-net of depth three, with 8, 16 and 32 filters along the contracting
825 path, was trained to predict cell interiors from phase contrast images. Phase contrast images
826 were normalized by subtracting the median and scaling to intensities expected between the
827 2nd and 98th percentiles. Cell interiors were defined from the curated outlines by filling each
828 outline and then subjecting it to two rounds of morphological erosion. The erosion step ensured
829 that neighbouring cells predicted by the network were well separated, such that distinct cell
830 instances could be clearly identified simply by thresholding the prediction and labelling

831 connected regions. After instance identification, two rounds of morphological dilation restored
832 each mask to its original size. Finally, a smooth outline for each cell was obtained as a two-
833 dimensional spline defined by equidistant knots placed on the mask edge.
834 To track cells between time points, we applied a length conservation strategy for the cells along
835 each trench. At each time point, we ordered cell outlines by their depth in the trench, with
836 deepest cells first. We then attempted to match, in order, a cell outline in time point *t* with one
837 or more cell outlines in time point *t*+1, chosen such that the sum of their cell lengths would be
838 conserved within some threshold tolerance. In the trivial case, the length of the first outline at
839 time point *t* would match that of the first outline at time point *t*+1. In the event of cell division,
840 the cell length at time point *t* would match the sum of the first two cell lengths at time point *t*+1.
841 Since cells may grow in length between time points, we also initialised a growth rate parameter
842 for each cell that biased the expected cell lengths for time point *t*+1 as a fold-increase in length.
843 To enable adaptation to the true growth rate, the growth rate parameter was updated by a
844 lagging average over 20 time points. To increase robustness to errors in segmentation, we
845 additionally allowed state transitions from one to many and many to one, and built a proposal
846 tree, which branched for all valid assignments lying within the length thresholds. We searched
847 for the proposal with the lowest average fold-change in matched lengths, but limited branching
848 by retaining only the 10 best proposals for subsequent nodes (cell outlines) in the tree. The
849 length thresholds were deliberately set loosely such that the (sum of) cell length(s) at *t*+1 could
850 decrease at most five-fold or increase at most two-fold relative to the (sum of) cell length(s) at
851 *t*. This increased the number of valid proposals, but was important in cases where the growth
852 rate estimate was poor. For transitions where one cell outline split into more than two, or
853 transitions where multiple outlines merged into one cell, a new label was generated for the
854 corresponding cells at *t*+1. We made one exception to this labelling strategy to account for
855 occasional ambiguity in segmentation near division events, where a cell segmented as two
856 sister cells could later be segmented as a single mother cell. Specifically, when two sister cells
857 — i.e., cells that were previously involved in a division event — merged into one, the label was
858 set back to that of the mother; at the next division event, the labels of the sister cells were also
859 retained. Finally, note that any outlines below a minimum size threshold of 50 pixels were
860 ignored. All errors in tracking were manually curated.
861 Cell length was estimated from cell regions as the 'major axis length' of the Matlab regionprops
862 function — the major axis of the ellipse with same normalised second central moment as the
863 region. Instantaneous growth rates were estimated from the derivative of a smoothing spline
864 fitted to the logarithm of cell length over each cell division cycle. Knots for the spline were
865 placed at intervals of at most 15 time points. Single-cell fluorescence traces were quantified
866 from the median fluorescence within each outline. Background fluorescence varied as a
867 function of time due to the accumulation of cells at some trench exits, so we corrected for

868 background fluorescence in each trench at each time point using the median value of all non-
869 cell pixels. Fluorescence traces were characterised along branching lineages and were
870 smoothed with a Savitzky-Golay filter of order 3 and window length 21. The derivative of the
871 filter was used to obtain the maximum rate of fluorescence increase. Peaks in fluorescence
872 were identified as points for which the second derivative was less than -100 and either the first
873 derivative was zero, or its sign changed at the next time point. In cases where multiple
874 descendants shared a common peak event before branching, we counted that event only once.
875 The half-life of decay after a peak in fluorescence was determined by fitting an exponential
876 decay function with offset term to fluorescence data after the peak. Given the occasional
877 occurrence of a second peak in fluorescence, the decay function was only fit to time points
878 after the peak up to the point where the first derivative exceeded zero.
879

880 1. Qin D, Xia Y, Whitesides GM. Soft lithography for micro- and nanoscale patterning. Nat
881 Protoc. 2010;5(3):491-502. Epub 2010/03/06. doi: 10.1038/nprot.2009.234. PubMed PMID:
882 20203666.
883 2. Ronneberger O, Fischer P, Brox T. U-net: Convolutional networks for biomedical image
884 segmentation. arXiv. 2015;[1505.04597].
885